Research Article

Identification and Preclinical Pharmacology of the γ-Secretase Modulator BMS-869780

Jeremy H. Toyn,[1] Lorin A. Thompson,[2] Kimberley A. Lentz,[3] Jere E. Meredith Jr.,[1] Catherine R. Burton,[1] Sethu Sankaranararyanan,[1] Valerie Guss,[1] Tracey Hall,[1,4] Lawrence G. Iben,[1] Carol M. Krause,[1] Rudy Krause,[1] Xu-Alan Lin,[1] Maria Pierdomenico,[1] Craig Polson,[1] Alan S. Robertson,[1] R. Rex Denton,[3] James E. Grace,[3] John Morrison,[3] Joseph Raybon,[3] Xiaoliang Zhuo,[3] Kimberly Snow,[3] Ramesh Padmanabha,[5] Michele Agler,[5,6] Kim Esposito,[5] David Harden,[5] Margaret Prack,[5] Sam Varma,[5,7] Victoria Wong,[5,8] Yingjie Zhu,[5,9] Tatyana Zvyaga,[5] Samuel Gerritz,[2] Lawrence R. Marcin,[2] Mendi A. Higgins,[2] Jianliang Shi,[2] Cong Wei,[10,11] Joseph L. Cantone,[10] Dieter M. Drexler,[10] John E. Macor,[2] Richard E. Olson,[2] Michael K. Ahlijianian,[1] and Charles F. Albright[1]

[1] *Exploratory Biology and Genomics, Bristol-Myers Squibb Research and Development, 5 Research Parkway, Wallingford, CT 06492, USA*

[2] *Discovery Chemistry, Bristol-Myers Squibb Research and Development, 5 Research Parkway, Wallingford, CT 06492, USA*

[3] *Pharmaceutical Candidate Optimization, Bristol-Myers Squibb Research and Development, 5 Research Parkway, Wallingford, CT 06492, USA*

[4] *Preclinical Sciences, Alexion Pharmaceuticals, Inc 352 Knotter Drive, Cheshire, CT 06410, USA*

[5] *Lead Discovery and Lead Profiling, Bristol-Myers Squibb Research and Development, 5 Research Parkway, Wallingford, CT 06492, USA*

[6] *High Throughput Biology, Boehringer Ingelheim, 900 Ridgebury Road, Ridgefield, CT 06877, USA*

[7] *Stratford High School, 45 North Parade, Stratford, CT 06615, USA*

[8] *External Research Solutions, WWMC, Pfizer World Wide Research & Development, Eastern Point Road, Groton, CT 06340, USA*

[9] *Arvinas Inc, 5 Science Park, New Haven, CT 06511, USA*

[10] *Discovery Analytical Sciences, Bristol-Myers Squibb Research and Development, 5 Research Parkway, Wallingford, CT 06492, USA*

[11] *Department of Pharmacokinetics, Dynamics and Metabolism, Pfizer World Wide Research & Development, Eastern Point Road, Groton, CT 06340, USA*

Correspondence should be addressed to Jeremy H. Toyn; toynhouse@aol.com

Alzheimer's disease is the most prevalent cause of dementia and is associated with accumulation of amyloid-β peptide (Aβ), particularly the 42-amino acid Aβ1-42, in the brain. Aβ1-42 levels can be decreased by γ-secretase modulators (GSM), which are small molecules that modulate γ-secretase, an enzyme essential for Aβ production. BMS-869780 is a potent GSM that decreased Aβ1-42 and Aβ1-40 and increased Aβ1-37 and Aβ1-38, without inhibiting overall levels of Aβ peptides or other APP processing intermediates. BMS-869780 also did not inhibit Notch processing by γ-secretase and lowered brain Aβ1-42 without evidence of Notch-related side effects in rats. Human pharmacokinetic (PK) parameters were predicted through allometric scaling of PK in rat, dog, and monkey and were combined with the rat pharmacodynamic (PD) parameters to predict the relationship between BMS-869780 dose, exposure and Aβ1-42 levels in human. Off-target and safety margins were then based on comparisons to the predicted exposure required for robust Aβ1-42 lowering. Because of insufficient safety predictions and the relatively high predicted human daily dose of 700 mg, further evaluation of BMS-869780 as a potential clinical candidate was discontinued. Nevertheless, BMS-869780 demonstrates the potential of the GSM approach for robust lowering of brain Aβ1-42 without Notch-related side effects.

1. Introduction

Alzheimer's disease (AD) is the most prevalent cause of dementia. More than 35 million people have dementia worldwide and the prevalence is expected to double in the next 20 years [1]. Medicines are available for treatment of symptoms but provide limited benefit and do not prevent AD [2]. The cause of AD is not completely understood, but a widely held view of its pathogenesis is based on the amyloid hypothesis. Accumulation and aggregation of the toxic amyloid-β peptide (Aβ), particularly the 42-amino acid form Aβ1-42 [3], initiates neuronal dysfunction that eventually leads to brain atrophy, dementia, and death [4, 5]. Aβ is naturally produced in the brain by proteolytic processing of a type I transmembrane protein, the amyloid-β precursor protein (APP). APP is processed by the β-site APP cleaving enzyme (BACE), releasing a secreted ectodomain and a membrane-anchored C-terminal fragment (APP-CTFβ). Subsequent cleavage of APP-CTFβ within the transmembrane domain by γ-secretase then produces a cytosolic intracellular domain (AICD) and Aβ, which is secreted. In addition, a fraction of APP is cleaved by α-secretase at a site within the Aβ sequence to produce APP-CTFα, which is subsequently cleaved by γ-secretase to produce nonamyloidogenic peptides [6]. Compounds targeting either BACE or γ-secretase have been tested in clinical trials, but adequate Aβ-lowering at tolerated doses in patients has been a challenge [7].

γ-Secretase is a lipid bilayer-embedded aspartyl protease consisting of four core subunits; nicastrin, Aph-1, Pen-2, and presenilin. Presenilin carries the active site aspartyl residues, whereas the other subunits play ancillary roles in enzymatic activity and maturation [6, 8, 9]. Structural studies of γ-secretase using electron micrographic image analysis and biochemical methods to map locations of amino acid residues suggest a compact structure with the active site contained within a hydrophilic chamber surrounded by transmembrane domains [10–14]. High resolution structure of γ-secretase has not been reported, but, based on analogy to X-ray crystallography of a presenilin homolog [15], it seems likely that the active site aspartates would be located within an intramembrane pore surrounded by the transmembrane domains of presenilin. The biological role of γ-secretase involves the proteolytic cleavage of transmembrane domains of at least 80 different protein substrates, including APP and the Notch family [16]. Although the physiological significance of substrate processing is unknown in most cases, γ-secretase cleavage of Notch and production of the Notch intracellular domain (NICD) are critical for adult cell differentiation in the immune system and gastrointestinal tract [17, 18]. Inhibitors of γ-secretase (GSI) can be effective for Aβ lowering; however Notch inhibition likely contributes to dose-limitation [19].

A class of small molecules that avoid Notch inhibition are the γ-secretase modulators (GSM), which, like GSIs, target presenilin [20–24]. In contrast to GSIs, which inhibit Aβ production, GSMs have relatively little overall effect on Aβ production. Instead, GSMs change the lengths of Aβ peptides produced, causing decreased amounts of longer peptides, such as Aβ1-40 and Aβ1-42, and increased amounts of shorter peptides, such as Aβ1-37 and Aβ1-38 [25]. GSMs have analogous effects on other γ-secretase substrates, including Notch, causing a shift from the longer Nβ1-25 to the shorter Nβ1-21 Notch-derived peptides [26, 27]. The shift from longer to shorter Aβ peptides was first described for several nonsteroidal anti-inflammatory drugs (NSAID), which have low potency GSM activity [28], and was subsequently found in other small molecules and natural products [25]. The effect of GSMs is thought to result from allosteric stimulation of the stepwise cleavage mechanism of γ-secretase. The stepwise mechanism initiates with an endopeptidic cleavage of APP-CTF near the cytosolic face of the lipid bilayer, at either position 48 or position 49 (using the conventional amino acid numbering starting at position 1 for the aspartyl residue at the N-terminus of Aβ). Subsequently, γ-secretase carries out a series of carboxypeptidase-like cleavages at three or four amino acid intervals thereby producing tripeptides or tetrapeptides and Aβ peptides of different lengths [29, 30]. Typically, the 40-amino acid long Aβ1-40 is the major product, but lesser amounts of other Aβ peptides such as Aβ1-38 and Aβ1-42 are also produced. For example, Aβ1-40 biogenesis appears to require four cycles of APP-CTF cleavage at positions 49, 46, 43, and 40, resulting in the release of three tripeptides and one AICD (amino acids 50–99) for each Aβ1-40 peptide produced. Likewise, production of the Aβ1-42 peptide is associated with a series of cleavages that start at position 48 of APP-CTF [30, 31]. In the presence of a GSM, γ-secretase carries out an increased number of carboxypeptidase cycles per molecule of APP-CTF substrate, resulting in shorter Aβ peptides without substantially affecting the overall amount of Aβ produced [27, 32].

Despite having low potency, NSAID GSMs such as flurbiprofen were reported to lower brain Aβ1-42 in rodents [33, 34]. However, in clinical trials, flurbiprofen (tarenflurbil) was found to have no effect on Aβ1-42 in cerebrospinal fluid even at high doses [35]. High potency GSMs have also entered early stage clinical trials, but effects on Aβ1-42 in cerebrospinal fluid have not been reported [36, 37]. Many further GSMs have been evaluated *in vitro* and in animal studies, which, like the NSAID GSMs, do not inhibit Notch or other γ-secretase substrates [25, 38–51]. In addition, chronic dosing of GSMs has been reported to ameliorate plaque pathology [39, 45, 52] and enhance cognition in APP transgenic mice [48, 52, 53]. Thus, GSMs are capable of lowering brain Aβ1-42 and are expected to avoid the dose limitations of GSIs that are due to Notch-related side effects. A number of studies have reported at least some of the systemic exposure data associated with brain Aβ1-42 lowering, thus giving an idea of active exposures and doses for GSM [39–42, 44–46, 52]. However, preclinical predictions relating to safety margins or human dose have not been reported. Furthermore, the active exposures and doses in rodents are high, making it a matter of conjecture whether or not any of the currently published GSMs are likely to exhibit adequate safety margins or clinically acceptable doses. Here we describe the pharmacological properties of the GSM BMS-869780, a potent bicyclic triazole GSM [54, 55], and the quantitative predictions of human dose and off-target side effects. While these outcomes prevented the development of BMS-869780, they put in perspective the
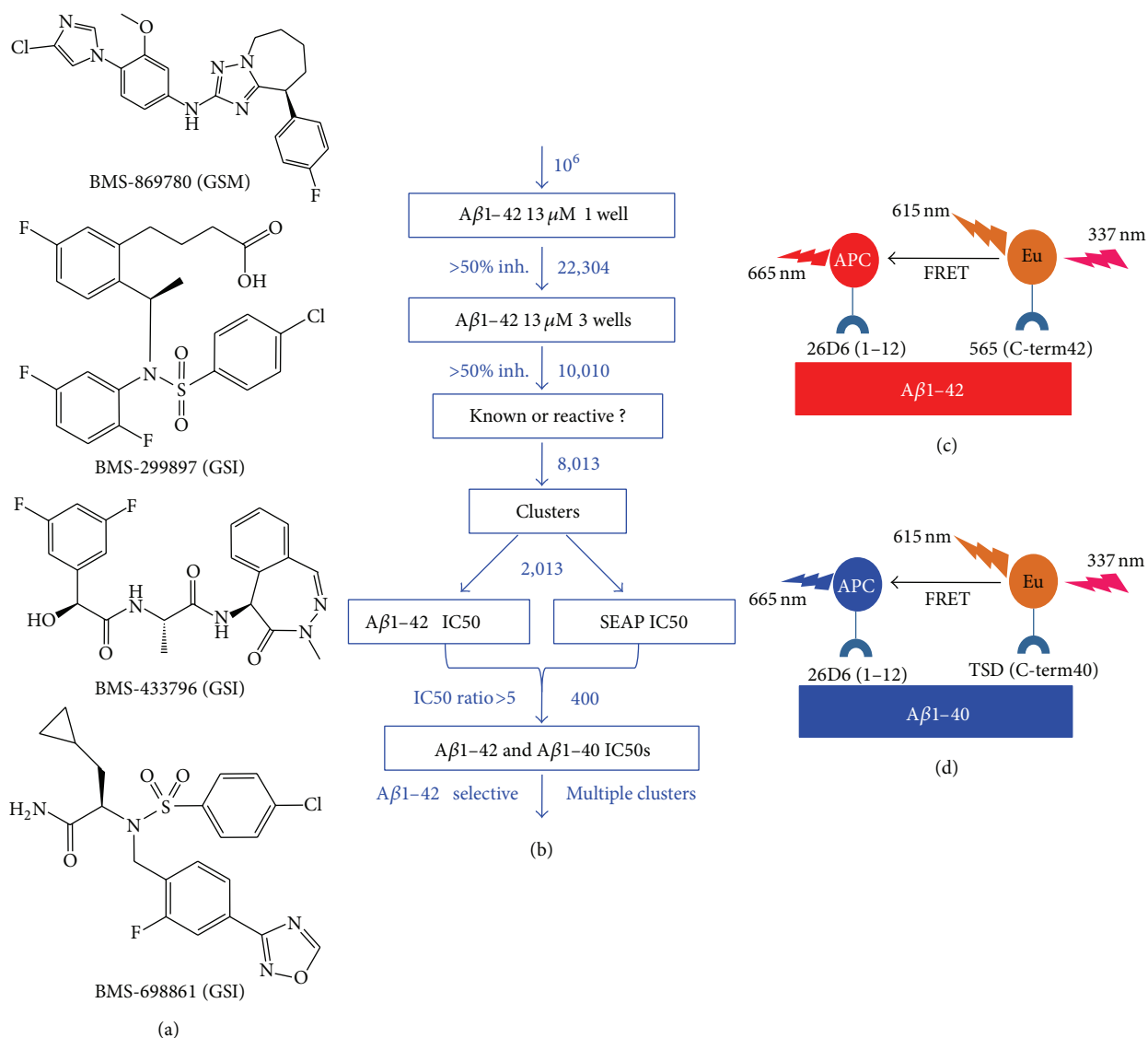
FIGURE 1: (a) Chemical structures of the compounds used in this study are shown. (b) Overview of the HTS and subsequent triage of compounds summarizes experimentation steps in boxes, with outcomes indicated beside the arrows. Costs of reagents and disposables were a major consideration in the design, particularly the initial screen of 10^6 samples. (c) Principle of the Aβ1-42 immunoassay; simultaneous binding of monoclonal antibody conjugates 252-APC and 565-Eu (specific for C-terminus of Aβ1-42) to Aβ1-42 leads to FRET-based emission at 665 nm. The ratio of emission at 665 nm to fluorescence at 615 nm represents the level of Aβ1-42 in the sample. (d) Principle of the Aβ1-40 immunoassay; same as described above for the Aβ1-42 immunoassay, except that the monoclonal antibody conjugate TSD-Eu (specific for C-terminus of Aβ1-40) was used in place of 565-Eu.

extent of further enhancements in drug-like properties that would be necessary to justify clinical testing of a future GSM.

2. Materials and Methods

2.1. Compounds. The GSM, BMS-869780 [54, 55], and the GSIs BMS-299897 [56] and BMS-433796 [57] have been reported previously. The GSI BMS-698861 is described in a BMS patent [58]. Chemical structures are shown in Figure 1(a).

2.2. Cell Cultures. H4-APPsw cell cultures were maintained on Dulbecco's modified Eagle's medium (DMEM) supplemented with L-glutamine (2 mM), fetal bovine serum (10%), and G418 (100 μg/mL). For IC$_{50}$ determinations, cells were harvested, resuspended in DMEM supplemented with 0.0125% bovine serum albumin, and dispensed into 384-well plates (1.5×10^4 cells per well). Aβ1-42 and Aβ1-40 assays, and Notch inhibition assays, were carried out as described previously [59]. Mouse embryonic fibroblasts deficient in PS1 and PS2 (MEF dKO) [60] were passaged twice per week in DMEM/F-12 medium, consisting of
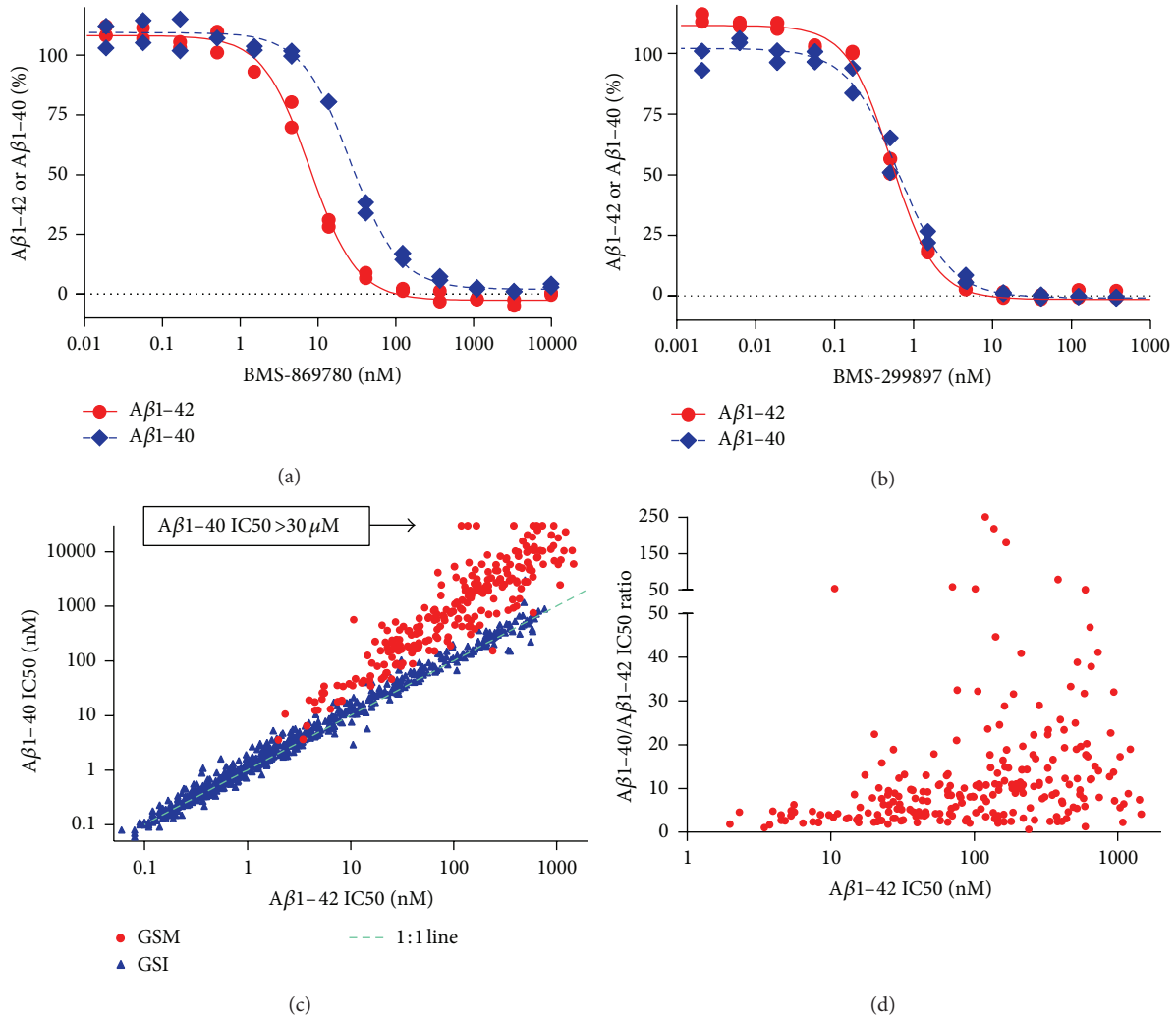
(a)

(b)

(c)

(d)

Figure 2: *In vitro* potency of BMS-869780 in the HTS assay. (a) H4-APPsw cultures were treated overnight with BMS-869780 (a GSM) at a range of concentrations and the relative levels of Aβ1-42 (red ●) and Aβ1-40 (blue ♦) were determined for calculation of IC$_{50}$ values (summarized in Table 1). (b) H4-APPsw cultures were treated overnight with BMS-299897 (a representative GSI) as described for BMS-869780 in panel (a). IC$_{50}$ values are summarized in Table 1. (c) IC$_{50}$ values for Aβ1-42 and Aβ1-40 lowering were determined for 236 GSM (red ●) and for 688 GSI that were mostly of the type containing the aryl sulfonamide core (blue ▲). For some compounds, the Aβ1-40 IC$_{50}$ value was greater than 30 μM, the highest concentration tested in the Aβ1-40 assay (arrow). (d) The ratio of the Aβ1-40 IC$_{50}$ to Aβ1-42 IC$_{50}$ was plotted against Aβ1-42 IC$_{50}$ for the same 236 GSM illustrated in (c).

a 1:1 mixture of DMEM and F-12 nutrient mixture supplemented with 10% fetal bovine serum, penicillin, and streptomycin. For expression of human presenilin-1 in MEF dKO cells, the full length human presenilin-1 cDNA open reading frame was cloned between the BamHI and XhoI sites of the vector pcDNA5/FRT (Invitrogen), placing presenilin-1 expression under the control of the CMV promoter. The M146V mutated allele was introduced into the presenilin-1 expression construct by polymerase chain reaction using the oligonucleotide primers 5′-CAGTGTCATTGTTGTCGTGACTATCCTCCTGGTGG-3′ and 5′-CCACCAGGAGGATAGTCACGACAACAATGAC ACTG-3′ (QuikChange kit, Invitrogen). MEF dKO cultures were cotransfected with DNA constructs expressing APP-CTF, encoding the C-terminal 99 amino acids of APP [61]

and either the human presenilin-1 or presenilin-1 M146V allele. Transfected cultures were incubated overnight at 37°C in 5% CO$_2$ atmosphere and then harvested, resuspended in DMEM/F-12 medium, dispensed into 96-well culture plates, and incubated for 6 hours at 37°C in 5% CO$_2$ atmosphere. Culture medium was then replaced with Ultraculture serum free medium (Lonza, Rockland, ME) with or without compounds at a range of concentrations and incubated overnight.

2.3. Aβ Antibodies and Conjugates. Anti-Aβ monoclonal antibodies and their epitopes used in this study were 4G8 (Aβ17-24; Covance), 252Q6 (rodent Aβ1-12; Invitrogen), D2A6H (Aβ37 C-terminal; Cell Signaling, catalog number

12356BF), TSD ($A\beta$40 C-terminal), 26D6 (human $A\beta$1-12), and 565 ($A\beta$42 C-terminal; Bristol-Myers Squibb). The covalent antibody-fluorophore conjugates were made at Perkin-Elmer, including TSD-Europium cryptate (TSD-Eu), 565-Europium cryptate (565-Eu), and 26D6-allophycocyanin (26D6-APC). Streptavidin-horseradish peroxidase (SA-HRP) and 4G8-biotin conjugates were from Covance. Horseradish peroxidase (HRP) conjugates of 565, 26D6 and 252Q6 (565-HRP, 26D6-HRP and 252Q6-HRP) were made using preactivated HRP (Easylink, Zymed/Invitrogen). The 6E10-sulfo-tag conjugate was from Mesoscale Discovery (catalog number K15148E-1), and the 252Q6-sulfo-tag conjugate was made using a kit (Mesoscale Discovery catalog number R91AN-1).

2.4. Immunoassays. IC_{50} determinations for $A\beta$1-42 and $A\beta$1-40 in H4-APPsw cultures in 384-well format were determined using homogeneous time-resolved fluorescence immunoassays as previously described [59]. The principle of these assays is illustrated in Figures 1(c) and 1(d). In other experiments using H4-APPsw cultures, $A\beta$ was quantified by ELISA; for $A\beta$1-42 the of monoclonal antibodies was 26D6 and 565-HRP; for $A\beta$1-40 it was TSD and 26D6-HRP, and for $A\beta$1-x it was 4G8 and 26D6-HRP. In some experiments a novel 4-plex $A\beta$ electrochemiluminescence immunoassay was used (Mesoscale Discovery catalog number N45ZA-1). Briefly, the 4-plex was carried out in 96-well format, with 4 separate spots of capture antibodies in each well. The 96-well plates were prepared by the manufacturer, with spots of monoclonal antibodies for $A\beta$1-42, $A\beta$1-40, and $A\beta$1-38, and an additional fourth spot of streptavidin in each well. Plates were initially incubated with blocking buffer (5% BSA in phosphate buffered saline, 200 μL per well) for 2 hours at ambient temperature and then with D2A6H-biotin conjugate (50 ng/mL in 1% BSA, phosphate buffered saline, 25 μL per well) for 1 hour. Plates were then rinsed with phosphate buffered saline before addition of experimental samples for determination of $A\beta$1-42, $A\beta$1-40, $A\beta$1-38, and $A\beta$1-37 levels, following the manufacturer's instructions as for the $A\beta$ 3-plex kit (catalog number K15148E-1). Rat brain extracts for use in the 4-plex assay were made in 0.2% diethylamine, as previously described [62]. For detection of rat $A\beta$ peptides in the 4-plex (Figure 5), 252Q6-sulfo-tag conjugate was used, and for detection of human $A\beta$ peptides from cell cultures 6E10-sulfo-tag conjugate was used. For $A\beta$ in transiently transfected PS1/PS2 dKO fibroblasts, $A\beta$1-42 was quantified using an ELISA kit (WACO), and $A\beta$1-40 was quantified by ELISA as described above for H4-APPsw cultures. For triple transgenic mice (3xTg; [63]), human transgenic $A\beta$1-42 was assayed in brain homogenates using an ELISA kit (WACO). For the rat and mouse experiments illustrated in Figures 7 and 8, brain samples were prepared by solid phase extraction [64], and endogenous rat brain $A\beta$1-42 and $A\beta$1-40 were quantified by ELISA as previously described for wild type mice [65]. For brain extracts made using solid phase extraction, calibration of $A\beta$ was relative, based on the approximately linear response of the assay in the range

tested. For brain extracts made in 0.2% diethylamine, $A\beta$1-42, $A\beta$1-40, $A\beta$1-38, and $A\beta$1-37 concentrations in brain and cell culture samples were determined by fitting the results of immunoassays against calibration curves derived from a range of dilutions of the corresponding synthetic peptides on each assay plate using a quadratic curve fit (Graphpad Prizm 5.0). $A\beta$1-x was calibrated in the same way against synthetic $A\beta$1-40 peptide. Results were expressed in units of pM, corrected for sample dilution.

2.5. Immunodepletion of $A\beta$. For immunodepletion of rat brain $A\beta$, solid phase extracts [64] were pooled within treatment groups. The pools were divided into equal aliquots and incubated with or without monoclonals 565, TSD, 4G8, or 6E10 (10 μg) at 4°C overnight. Protein G beads (50 μL; EZview, Sigma) were added, and incubation was continued with agitation for 1 hour. The beads were removed by centrifugation, and $A\beta$1-40 and $A\beta$1-42 in the unbound fraction were quantified by ELISA, as described above.

2.6. Western Blotting. For western blotting of $A\beta$ peptides from H4-APPsw cell cultures, $A\beta$ was immunoprecipitated directly from the cell culture medium and was eluted from the protein G beads by addition of lithium dodecyl sulfate (LDS) electrophoresis sample buffer (Invitrogen). $A\beta$ peptides were separated by gel electrophoresis in the presence of 8 M urea [66], transferred to PVDF membrane, and detected by western blotting using monoclonal 26D6-HRP conjugate.

For western blotting of APP-CTF in cell lysates, H4-APPsw cell cultures in T-75 flasks were rinsed with DPBS, harvested, isolated by centrifugation, and stored at −80°C until needed. Cells were suspended in SDS sample buffer (20,000 cells/μL), boiled for 10 min, and centrifuged 3000 ×g for 5 min. Total protein content was determined using an assay kit (EZQ, Invitrogen cat number R33200). Proteins were separated by electrophoresis on Bis-Tris 16% polyacrylamide gels and transferred to nitrocellulose filters. APP-CTFβ was detected using 26D6-HRP, and APP-CTFα was detected using ct695 polyclonal (Invitrogen, cat number 51-2700) and secondary goat anti-rabbit horseradish peroxidase conjugate (Zymed, catalog number 62-6120). Chemiluminescence images were captured and quantified using an imaging station (Fuji model number LAS-3000). The ct695 western blots also show APP-CTFβ, which migrates as a fainter band above APP-CTFα under these conditions. To confirm the consistency of sample loading, the APP-CTF western blots were reprobed for glyceraldehyde-3-phosphate dehydrogenase (GAPDH) using monoclonal 1D4 (Enzo Life Sciences, cat number CSA-335).

For immunoprecipitation and western blotting of APP-CTFβ and APP-CTFα from rat brain, weighed sagittal brain halves were homogenized using a rotary homogenizer (Polytron) in 5 volumes of RIPA buffer (Sigma R-0278; 150 mM NaCl, 1.0% IGEPAL CA-630, 0.5% sodium deoxycholate, 0.1% SDS, 50 mM Tris, pH 8.0) containing protease inhibitors (Roche complete cat number 11836145001) and centrifuged at 25,000 ×g for 30 min. All steps were carried out on ice or at 4°C. The pellet from centrifugation was

discarded. Total protein concentration in the supernatant was determined using BCA protein assay (Pierce number 23227), and all samples were adjusted to a concentration of 18 mg/mL by addition of RIPA buffer. For APP-CTFβ immunoprecipitation, 5 μg of 252Q6 was added to 1 mL of homogenate and incubated on ice for 1 hour, and then 50 μL of magnetic protein A/G beads (Thermo Scientific cat number 88803) was added, and incubation was continued overnight with mixing. Using a magnet to isolate the beads, beads were washed once with 1 mL RIPA and twice with 1 mL of Tris saline pH 7.5 (50 mM Tris pH 7.5, 15 mM NaCl). The beads were resuspended in 40 μL of SDS sample buffer, boiled 5 mins, and removed using the magnet before gel electrophoresis and western blotting using ct695 polyclonal, as described above. For APP-CTFα, 5 μg of 4G8 was added to homogenates previously used for immunoprecipitation of APP-CTFβ, and immunoprecipitation using magnetic beads followed by western blotting using ct695 polyclonal was carried out as described above.

2.7. Mass Spectrometry of Aβ Peptides from Cell Cultures. H4-APPsw cell cultures were grown in T-75 flasks until 75% confluent and rinsed with Dulbecco's phosphate buffered saline (DPBS; Gibco cat number 14109), and 20 mL of DMEM supplemented with L-glutamine (2 mM), geneticin, penicillin, streptomycin, and DMSO with or without BMS-869780 was added (final concentration of DMSO was 0.2%). After incubation for 24 hours at 37°C in 5% CO_2, culture medium was removed, centrifuged to remove cells, and frozen in aliquots at −80°C. For immunoprecipitation, aliquots of cell medium (4 mL) were thawed, followed by the addition of protease inhibitor cocktail (Sigma P-8340) to a final concentration of 1%, 60 ng of [^{15}N]-Aβ1-40 synthetic peptide (rPeptide, 1101-1, Athens, GA), 30 μg of monoclonal 26D6, and 15 μg of monoclonal 4G8. After incubation for 20 min on ice, 80 μL of protein G agarose beads (Pierce Rockford, IL) was added, and incubation was continued overnight at 4°C. Beads were isolated by centrifugation and washed three times by centrifugation in 1 mL of ice cold phosphate buffered saline and then washed a final time in 1 mL 10 mM Tris-HCl pH 8.0. Aβ was eluted from the beads using 30 μL of 70% acetonitrile/0.1% formic acid. MALDI-TOF MS analysis was conducted using a Bruker Ultraflex III TOF/TOF mass spectrometer (Billerica, MA). A mix of Aβ standard peptides (AnaSpec, Fremont, CA) Aβ1-37 ([M+H]$^+$ = m/z 4071.5), Aβ1-38 ([M+H]$^+$ = m/z 4128.5), Aβ1-39 ([M+H]$^+$ = m/z 4227.7), Aβ1-40 ([M+H]$^+$ = m/z 4326.9), Aβ1-42 ([M+H]$^+$ = m/z 4511.2), and [^{15}N]Aβ1-40 ([M+H]$^+$ = m/z 4378.4) was prepared to a final concentration of 1 ng/μL in 50 : 50% acetonitrile : water (v : v). Both the standard peptide sample and the samples from H4-APPsw cell medium following immunoprecipitation (IP) were further processed by mixing 5 μL sample with 5 μL of 7 mg/mL MALDI matrix (α-cyano-4-hydroxycinnamic acid, CHCA, from Sigma-Aldrich, St. Louis, MO) in 70 : 30% acetonitrile : water (v : v) with 0.1% trifluoroacetic acid (v : v). 0.5 μL of sample was spotted to an Anchorchip 384-well target plate (Bruker Daltonics, Billerica, MA) and allowed to dry in air before analysis. Analysis of

various Aβ peptide isoforms from the standard peptides and the cell samples was performed in positive linear mode, accumulating 2000 spectra. Intensities of each analyte were normalized against a MALDI matrix peak (m/z 824.8) and the internal standard peak ([^{15}N]Aβ1-40, m/z 4378.4).

2.8. Notch Signaling and Processing Assays. Inhibition of Notch signaling in cultured cells using a mouse-derived truncated Notch1 transgene, mNotch-ΔE [67], has been described in detail previously [59]. Western blots for mNotchΔ1865 and NICD using 9E10 anti-c-myc monoclonal were carried out as previously described [68].

2.9. Animals and Dosing. All experimental procedures with animals followed National Institutes of Health guidelines and were authorized by and in compliance with policies of the Bristol-Myers Squibb Animal Use and Care Committee. Mice and rats were housed with a 6:00 AM to 6:00 PM light/dark cycle and allowed free access to food and water. For 3xTg mice [63], BMS-869780 was dosed in three-month-old females by oral gavage at 6 mL/kg in vehicle consisting of 84% polyethylene glycol average molecular weight of 400 (PEG-400), 15% EtOH, and 1% Tween-80 (w/w/w). The compound was dissolved in EtOH and then diluted with PEG-400 and Tween, after which the vial was sealed, vortexed, and sonicated at 56°C for 1 hour. Animals were euthanized by asphyxiation in CO_2. Blood was collected by cardiac puncture and placed into ethylene-diaminetetraacetic acid microtainer tubes for the preparation of plasma. The cerebellum was collected for the determination of compound concentration, and the remaining brain was separated into left and right halves before freezing in liquid nitrogen. For the rat time course study, 8- to 12-week-old female Sprague-Dawley rats were obtained from Charles River Laboratories (Wilmington, MA), BMS-869780 was dosed orally at 4 mL/kg, and brain and plasma samples were collected as described for the 3xTg mice. For the four day repeat dose rat study, BMS-869780 was given by oral gavage in vehicle consisting of PEG-400, PEG-200, D-α-tocopheryl polyethylene glycol succinate, Solutol HS 15, in the ratio 80 : 10 : 5 : 5 (w/w/w/w). Methods for the pharmacokinetics studies in rat, dog, and monkey are described below.

2.10. Pharmacokinetic to Pharmacodynamic (PK/PD) Relationship in Rodents. The data generated in the mouse and rat time course experiments were analyzed sequentially by nonlinear regression (WinNonlin Pharsight Corporation, Mountain View, CA). The pharmacokinetic data were best described by a 1-compartment linear model with first-order absorption and elimination. Subsequently, the pharmacodynamic parameters were estimated from the BMS-869780 plasma concentrations and the observed reductions of brain Aβ1-42 or Aβ1-40 by fitting to the equation for inhibition of synthesis [69]. The goodness-of-fit was determined by visual inspection, Akaike Information Criterion, Schwartz Criterion, examination of the residuals and the coefficient of variation of the parameter estimates.

2.11. Pharmacokinetics. Male Sprague-Dawley (SD) rats (300–350 g) were fasted overnight, and three per group received BMS-869780 either as an intravenous (IV) infusion in PEG400 : ethanol (90 : 10 w/w) at 1 mg/kg over 5 min via the jugular vein or as nanosuspension (d_{50} ca. 300 nm) by oral gavage at 5 mg/kg in Povidone K-30 : sodium lauryl sulfate : water (2.5 : 0.12 : 97.38 w/w/w/w). For the IV infusion, serial blood samples were obtained before dose and at 0.17, 0.25, 0.5, 0.75, 1, 2, 4, 6, 8, and 24 hours after dose. For the PO nanosuspension, serial blood samples were obtained before dose and at 0.25, 0.5, 0.75, 1, 2, 4, 6, 8, and 24 h after dose. Blood samples, ~0.3 mL, for all studies were collected from the jugular vein into K_3EDTA-containing tubes and then centrifuged at 4°C (1500–2000 ×g) to obtain plasma, which was stored at −20°C until analysis by LC/MS/MS. In male beagle dogs, the PK of BMS-869780 was evaluated in a cross-over study design with a one-week washout between treatments. Dogs were fasted overnight, and three animals (9.5 to 10.7 kg) received BMS-869780 by IV infusion at 1 mg/kg over 5 minutes in PEG400 : ethanol (90 : 10 w/w) or as nanosuspension (d_{50} ca. 300 nm) by oral gavage at 5 mg/kg in Povidone K-30 : sodium lauryl sulfate : water (2.5 : 0.12 : 97.38 w/w/w/w). Serial blood samples (~0.3 mL) were collected from a saphenous vein into K_3EDTA-containing tubes before dose and at 0.083, 0.17, 0.25, 0.5, 0.75, 1, 2, 4, 6, 8, and 24 hours after IV dose, and 0.25, 0.5, 0.75, 1, 2, 4, 6, 8, and 24 hours after oral dose, followed by centrifugation at 4°C (1500 to 2000 ×g) to obtain plasma. Samples were stored at −20°C until analysis of BMS-869780 levels by LC-MS/MS. In male cynomolgus monkeys, the PK of BMS-869780 was evaluated in a cross-over study design with a 1-week washout between treatments. Following an overnight fast, three animals (4.5 to 8 kg) received BMS-869780 by IV infusion via a femoral vein at 1 mg/kg over 10 minutes in PEG400 : ethanol (90 : 10), or by oral gavage at 5 mg/kg in Povidone K-30 : sodium lauryl sulfate : water (2.5 : 0.12 : 97.38). Serial blood samples, ~0.3 mL, were collected from a femoral artery into K_3EDTA-containing tubes before dose and at 0.083, 0.17, 0.25, 0.5, 0.75, 1, 2, 4, 6, 8, and 24 hours after IV dose, and 0.25, 0.5, 0.75, 1, 2, 4, 6, 8, and 24 hours after oral dose, followed by centrifugation at 4°C (1500 to 2000 ×g) to obtain plasma. Samples were stored at −20°C until analysis of BMS-869780 levels by LC-MS/MS. The PK parameters of BMS-869780 were obtained by noncompartmental analysis of plasma concentration versus time data (WinNonlin software, Version 5.0; Pharsight Corporation, Mountain View, CA). The peak concentration (C_{max}) and time for C_{max} (T_{max}) were recorded directly from experimental observations. The area under the curve from time zero to the last sampling time (AUC^{0-T}) and the area under the curve from time zero to infinity (AUC^{INF}) were calculated using a combination of linear and log trapezoidal summations. The total plasma clearance (CLTp), steady-state volume of distribution (Vss), apparent elimination half-life ($T_{1/2}$), and mean residence time (MRT) were estimated after IV administration. The absolute oral bioavailability (F) was estimated as the ratio of dose-normalized AUC values following oral and IV doses.

2.12. Prediction of Human Dose. Interspecies allometric scaling adjusted for brain weight was used to predict human CLTp [70], while simple allometric scaling was used to predict Vss [71]. Briefly, the Vss and brain weight adjusted CLTp values from nonclinical species were plotted against body weight on a log-log scale to yield estimates of Vss and CLTp × brain weight in humans. The estimated CLTp × brain weight for human was adjusted for the brain weight of humans to yield a predicted CLTp. All of the nonclinical species demonstrated mono- or biexponential plasma concentration-time profiles; therefore, the MRT method was used to simulate the human pharmacokinetic profile as described below. Noncompartmental analysis was performed using WinNonlin software (version 5.0; Pharsight Corporation, Mountain View, CA). The k_a for each species was obtained from the IV and PO (nanosuspensions) of rat, dog, and cynomolgus monkey by deconvolution of plasma concentration-time data using Kinetica (version 5.0; Seattle, WA). The bioavailability was estimated from the nanosuspensions from rat, dog, and cynomolgus monkeys. The average k_a and F, along with the Vss and CLTp from allometric scaling, were incorporated into a two-compartment model to predict the human oral plasma concentration-time profiles. Human steady state doses to achieve plasma AUCs comparable to those in rats which produced 25% ABEC (area between baseline and Aβ effect-time curve) reductions were estimated. The results are summarized in Tables 3 and 4.

2.13. Determination of BMS-869780 Concentrations. Plasma and brain samples were analyzed using an ultraperformance liquid chromatography-tandem mass spectrometry (UPLC-MS-MS) method. The UPLC MS-MS system consisted of a Waters Aquity Ultra Performance LC Sample Organizer, Solvent Manager and Sample Manager, a Waters BEH C18, 1.7 u 50 × 2.1 mm, column operated at 60°C, and a SCIEX API 4000 Q trap mass spectrometer. The mobile phase consisted of (A) water with 0.1% formic acid and (B) acetonitrile with 0.1% formic acid, delivered at 600 μL/min using a gradient program. The initial elution condition was 5% B which was maintained for 0.2 min and increased to 95% B in 0.5 min and maintained for 0.4 min. It was then returned to 5% B in 0.1 min and maintained for 0.2 min. The MS-MS analysis was performed using the heated nebulizer under positive ion mode with the source temperature at 400°C. The capillary voltage was 5000 eV and the collision energy 49 eV. The mass-to-charge ratios of 453 (precursor ion) and 438 (product ion) were used for multiple reaction mode monitoring of BMS-869780. The quantitation range for BMS-869780 was 1 to 5000 nM. Plasma samples were deproteinized and extracted with four portions of acetonitrile. Brain samples (0.1 g) were homogenized in 0.4 mL of acetonitrile.

2.14. Other Methods. Determination of IC_{50} values for inhibition of secreted alkaline phosphatase (SEAP) was carried out using an H4 cell line stably expressing SEAP. Cells were treated overnight with compounds in 384-well format, and SEAP accumulation in the culture media was quantified using a chemiluminescence substrate. The pregnane-X-receptor

transactivation assay (PXR-TA) was based on the methods of Goodwin et al. [72] as described previously [59]. In the 4-day rat study with BMS-869780, tissues were fixed in 10% neutral buffered formalin, embedded in paraffin, sectioned, stained with hematoxylin and eosin, and examined by light microscopy.

3. Results

3.1. Identification of BMS-869780. The first compounds reported to have GSM activity were NSAIDs that exhibited selective inhibition of Aβ1-42 production [28]. A high throughput screen (HTS) was therefore carried out using FRET-based immunoassays for Aβ1-42 and Aβ1-40 levels in H4-APPsw cultures. Approximately 10^6 compound samples were incubated for 24 hours in H4-APPsw cell cultures, one compound per well in 384-well format, at a single concentration of 13 μM. The 22,304 samples exhibiting greater than 50% inhibition of Aβ1-42 were subsequently retested in triplicate, that is, three additional wells at 13 μM. This yielded 10,010 samples for which the average inhibition of Aβ1-42 in the four test wells was greater than 50%. After elimination of some samples due to previously known Aβ inhibition or chemical reactivity, 8,013 compounds were organized into clusters of related structures based on structural similarities [73], and 2,013 representative compounds were chosen for further evaluation. To rule out nonspecific effects on production or secretion of Aβ, dose response curves were determined for secreted alkaline phosphatase (SEAP) and for Aβ1-42 to compare the IC$_{50}$ values. This yielded 409 samples that were relatively selective for Aβ1-42 (using a cutoff of $\geq$5-fold SEAP/Aβ1-42 IC$_{50}$ ratio). To assess possible selectivity for Aβ1-42 lowering, IC$_{50}$ values were determined in parallel for Aβ1-42 and Aβ1-40 in ca. 400 samples, and a series of compounds was identified from which BMS-869780 was subsequently derived through iterative improvements in potency and off-target profiles [54, 55]. An outline of the screening tiers and results obtained is shown in Figure 1(b), and the principle of the Aβ assays is shown in Figures 1(c) and 1(d).

3.2. Potency of BMS-869780 and Related Compounds for Aβ1-42 and Aβ1-40-Lowering. While many of the ca. 400 samples showed wide separations between the Aβ1-42 and Aβ1-40 IC$_{50}$ values, BMS-869780 itself showed only a four-fold separation between the IC$_{50}$ values (Figure 2(a)), presenting a minimal contrast with GSIs such as BMS-299897 (Figure 2(b)) and BMS-433796 (see summary of IC$_{50}$ values in Table 1). Nevertheless, as a group, compounds chemically related to BMS-869780 showed limited overlap with GSIs based on the separation of Aβ1-42 and Aβ1-40 IC$_{50}$ values, as illustrated for 236 GSMs and 688 GSIs (Figure 2(c)). This implies different Aβ-lowering mechanisms between the two groups. The ratios between Aβ1-42 and Aβ1-40 IC$_{50}$ values in the GSM group ranged from little more than two-fold to almost 250-fold, with a trend toward lower ratios for compounds with lower IC$_{50}$ values (Figure 2(d)). Anticipating subsequent experiments in the 3xTg mouse, the effect of the

presenilin M146V FAD mutant on BMS-869780 potency was evaluated. MEF cell cultures lacking endogenous presenilins were therefore cotransfected with human APP-CTFβ and human presenilin, either wild type or M146V allele. The IC$_{50}$ for Aβ1-42 was ca. 3-fold higher in cultures expressing the M146V allele, relative to cells expressing wild type presenilin. Likewise, Aβ1-40 IC$_{50}$ values were ca. 3-fold shifted, although the IC$_{50}$ appeared lower for Aβ1-40 in the wild type MEF cell cultures than in the H4-APPsw cultures. Thus, BMS-869780 appeared to be a little less potent in the context of the presenilin-1 M146V allele. IC$_{50}$ values are summarized in Table 1.

3.3. Evidence for the Noninhibitory Mechanism of BMS-869780 In Vitro. BMS-869780 showed only a 4-fold shift in IC$_{50}$ values between Aβ1-42 and Aβ1-40. The effect of BMS-869780 on Aβ1-37 and Aβ1-38 was therefore evaluated, as a more diagnostic test of the GSM mechanism [25]. H4-APPsw cultures were treated overnight with BMS-869780, and Aβ peptides were evaluated by mass spectrometry and western blotting. Using MALDI mass spectrometry, Aβ1-37, Aβ1-38, and Aβ1-40 were readily detected in vehicle-treated cultures, although Aβ1-42 levels were near the limit of quantitation. After treatment with BMS-869780 (100 nM), Aβ1-37 and Aβ1-38 were dramatically increased, whereas Aβ1-40 and Aβ1-42 were essentially undetectable (Figure 3(a)). The same conclusion was reached in experiments using a western blot method that separates different forms of Aβ. Increased levels of the shorter Aβ1-37 and Aβ1-38 peptides, which migrate more slowly than Aβ1-40 or Aβ1-42 by this method, were observed in cultures treated with BMS-869780 at 100 nM and 10 nM (Figure 3(b), lanes 3 and 4, resp.). Thus, taking the experimental data illustrated in Figures 2 and 3 together, BMS-869780 increased Aβ1-37 and Aβ1-38, while decreasing Aβ1-40 and Aβ1-42. This suggested that BMS-869780 would have a minimal effect, if any, on APP-CTFα and APP-CTFβ turnover. H4-APPsw cell cultures were therefore treated at high concentrations, relative to the IC$_{50}$s, of BMS-869780 and the GSI BMS-299897. For APP-CTFα, BMS-299897 caused an 8-fold increase in APP-CTFα, whereas BMS-869780 showed a 1.4-fold increase, averaged across doses (Figure 4(a)). The two compounds also showed a dramatic contrast in their effects on Aβ under these conditions. Whereas the GSI BMS-299897 dramatically reduced all Aβ1-x peptides, including Aβ1-42 and Aβ1-40, BMS-869780 selectively lowered Aβ1-42 and Aβ1-40, without any decrease in the overall levels of Aβ1-x (Figure 4(b)). In contrast to the result for APP-CTFα, APP-CTFβ levels were not affected in this experiment by either compound (Figure 4(a)), suggesting that γ-secretase was not a major pathway for APP-CTFβ turnover under these conditions. Indeed, it was recently reported that APP-CTFβ turnover in H4 cells occurs largely through proteasomal and lysosomal pathways, in contrast to APP-CTFα turnover which is more dependent on γ-secretase [74]. Thus, the effect of BMS-869780 on APP-CTFβ could not be directly evaluated in the H4-APPsw cell line under these conditions. To address the effect of BMS-869780 on APP-CTFβ, experiments were carried out in the context of the intended target organ, that
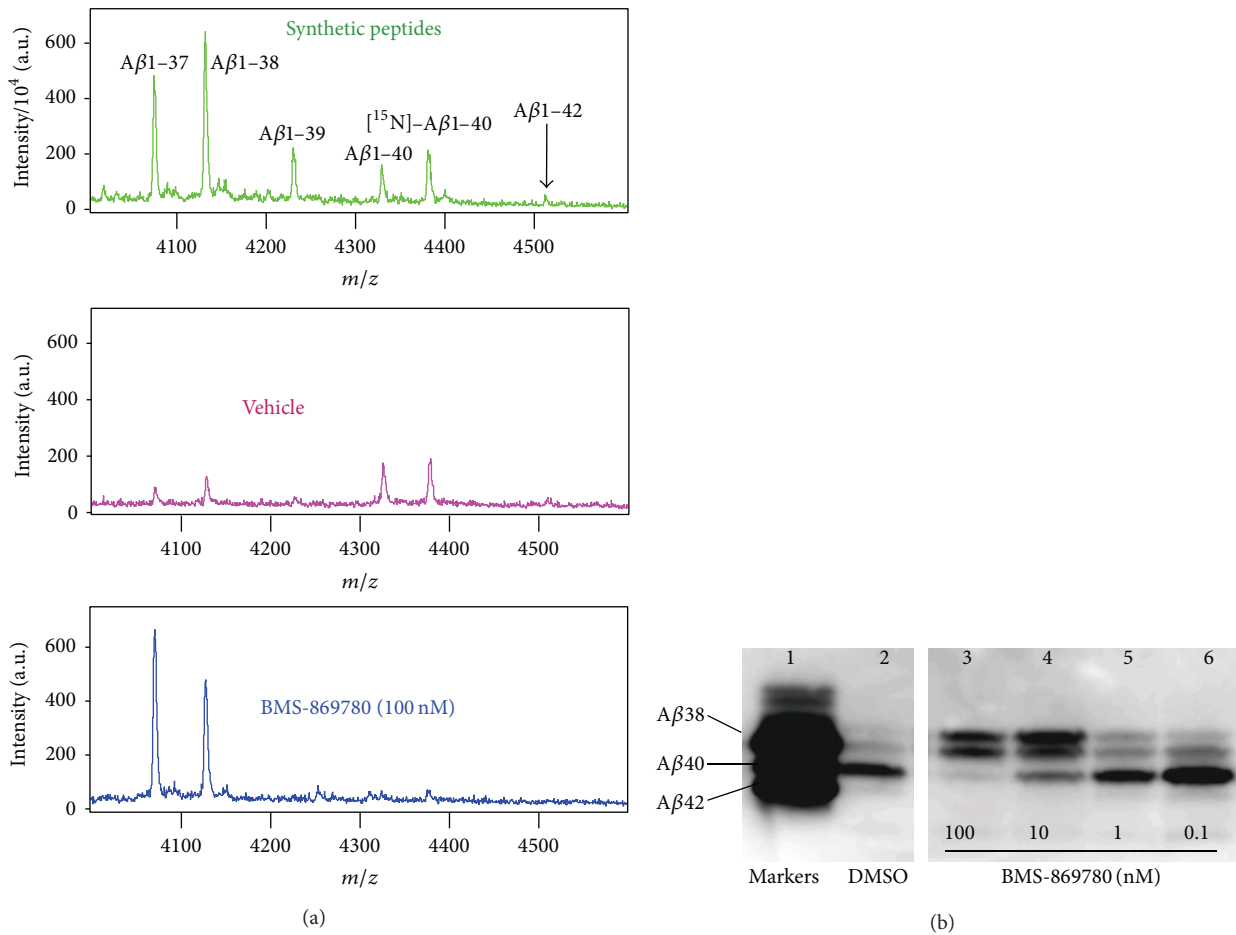
(a)

(b)

FIGURE 3: BMS-869780 increased the levels of the shorter peptides Aβ1-38 and Aβ1-37. (a) Top panel: an equimolar mix of synthetic peptides Aβ1-37, Aβ1-38, Aβ1-39, Aβ1-40, [^{15}N]-Aβ1-40, and Aβ1-42 was evaluated by MALDI-TOF mass spectrometry. H4-APPsw cell cultures were treated with vehicle (0.1% DMSO—middle panel) or BMS-869780 (100 nM—bottom panel), [^{15}N]-Aβ1-40 was added, and Aβ peptides were immunoprecipitated and evaluated by MALDI-TOF mass spectrometry. (b) H4-APPsw cell cultures were treated with BMS-869780 or DMSO vehicle. Aβ peptides were separated by gel electrophoresis in the presence of urea and detected by western blotting. Under these conditions, higher molecular weight Aβ peptides exhibit greater gel mobility. Lane 1: an equimolar mix of synthetic peptides Aβ1-38, Aβ1-40, and Aβ1-42. Lane 2: DMSO vehicle-treated cell culture. Lanes 3–6: Cell cultures treated with BMS-869780 at final concentrations of 100, 10, 1 and 0.1 nM, respectively.

TABLE 1: Aβ and Notch IC$_{50}$ values.

Assay (cell line)	BMS-869780 (GSM)			BMS-299897 (GSI)			BMS-433796 (GSI)		
	IC$_{50}$ (nM)	sd	n	IC$_{50}$ (nM)	sd	n	IC$_{50}$ (nM)	sd	n
Aβ1-42 (H4-APPsw)	5.1	2.2	13	0.47	0.61	322	0.16	0.08	256
Aβ1-40 (H4-APPsw)	24.1	7.7	7	1.3	1.2	93	0.19	0.14	20
Aβ1-42 (MEF PS1wt)	7.7	2.3	2						
Aβ1-40 (MEF PS1wt)	11	4	2						
Aβ1-42 (MEF M146V)	22	1.4	2						
Aβ1-40 (MEF M146V)	34	9	2						
mNotch1ΔE (luciferase)	>10000		3	340	108	147	2.1	1.0	256
mNotch1ΔE/Aβ1-42	>1785x			723x			13x		

is, in the brain of rats given oral doses of BMS-869780. The GSI BMS-698861 was dosed for comparison. BMS-869780 decreased Aβ1-40 and Aβ1-42 and increased Aβ1-37 and Aβ1-38 in rat brain. The sum total of Aβ1-40, Aβ1-42, Aβ1-38, and Aβ1-37 suggested no significant change in overall Aβ levels (Figure 5(a)). This was consistent with results obtained in the Aβ1-x assay, which showed no significant decrease despite the robust decrease in Aβ1-42 (Figure 5(b)). In contrast, BMS-698861 decreased levels of all the peptides, Aβ1-40, Aβ1-42, Aβ1-38, Aβ1-37, and Aβ1-x (Figures 5(a) and 5(b)). APP-CTFβ and APP-CTFα in samples of the same rat brains were evaluated by immunoprecipitation and western blotting. Neither APP-CTFβ nor APP-CTFα levels were affected in rats given BMS-869780, whereas levels of both peptides increased several-fold in rats given the GSI BMS-698861 (Figures 5(c)–5(f)). Thus, in brain, inhibition of γ-secretase by BMS-698861 resulted in APP-CTFβ and APP-CTFα accumulation, whereas modulation of Aβ by BMS-869780 had no effect on APP-CTFβ or APP-CTFα levels.

3.4. BMS-869780 Does Not Inhibit Notch Processing. The effect of BMS-869780 on Notch processing was evaluated using transcriptional reporter assays and western blotting of NICD levels. HeLa cell cultures were transfected with mNotch1ΔE and CBF1-luciferase reporter constructs and treated with BMS-869780. In most replicates of this experiment, inhibition of luciferase reporter occurred with IC$_{50}$ > 10 μM. In contrast, the GSIs BMS-299897 and BMS-433796 robustly inhibited luciferase activation, with IC$_{50}$ = 340 nM and 2.1 nM, respectively (Figure 6(a)). The IC$_{50}$ values for Notch-dependent luciferase expression are summarized in Table 1. To further evaluate the effect of BMS-869780 on Notch processing, western blots of cell cultures were carried out using mNotch1Δ1865, a truncated version of mNotch1ΔE that facilitates separation of NICD product from mNotch1 substrate on western blots [68]. HeLa cell cultures were transfected with mNotch1Δ1865 and treated overnight with compounds before western blotting. BMS-869780 had no effect on NICD levels at concentrations up to 3 μM, whereas the GSIs, BMS-299897, and BMS-433796, greatly reduced NICD (Figure 6(b)). Furthermore, the GSIs caused an increased level of mNotch1Δ1865 substrate, most likely due to inhibition of its turnover by γ-secretase, as previously noted by Blat et al. [68]. In contrast, 10 μM BMS-869780 did not increase mNotch1Δ1865 levels (Figure 6(b)), suggesting that the concomitant loss of NICD at 10 μM was due to a nonspecific effect, rather than inhibition of mNotch1Δ1865 turnover. This was also consistent with the observation of detached and dead cells in the presence of 10 μM BMS-869780.

3.5. Evaluation of BMS-869780 PK/PD and Residual Levels of Aβ. To evaluate BMS-869780 PK/PD, rats were given BMS-869780 intraperitoneally at a range of doses from 0.3 mg/kg to 100 mg/kg. The GSI BMS-698861 was dosed at 30 mg/kg for comparison. Five hours after dosing, brain Aβ1-42 and brain Aβ1-40 exhibited dose-dependent lowering with ca. 50% lowering at 3 mg/kg, and plasma Aβ1-40 lowering was dose dependent with ca. 50% lowering at 0.3 mg/kg

(Figure 7(a)). In contrast, brain Aβ1-x levels were not affected by BMS-869780 (Aβ1-x was evaluated only in samples from the highest three doses). For comparison, the GSI, BMS-698861, caused robust lowering in all Aβ assays, including Aβ1-x (Figure 7(a)). The concentration of BMS-869780 in plasma associated with 50% lowering of brain Aβ1-42 was ca. 1 μM (Figure 7(c)). Aβ1-42 appeared to be less completely inhibited than Aβ1-40. The linear correlation of Aβ1-42 with Aβ1-40 showed an intercept of 19.4% on the Aβ1-42 axis (Figure 7(b)), indicating a higher assay signal for Aβ1-42 relative to Aβ1-40 under conditions of maximal inhibition. Furthermore, at high plasma concentrations of BMS-869780, the best fit curve suggested a residual 29% Aβ1-42 and 11% Aβ1-40 assay signal remaining (Figure 7(c)). To investigate the residual assay signal further, brain Aβ1-42 and brain Aβ1-40 were evaluated in rats given four daily doses of BMS-869780 to achieve high sustained exposures, and residual levels of brain Aβ1-42 and Aβ1-40 were evaluated by immunodepletion. Despite the high exposures achieved (Table 4) and the extended time period in this experiment, residual ELISA signals for Aβ1-42 of 31% and for Aβ1-40 of 19% were observed (Figures 7(d) and 7(e)). Immunodepletion of the samples prior to ELISA was carried out to determine how much of the assay signal was due to residual Aβ1-42 or Aβ1-40. Specific monoclonals 565 and TSD selectively depleted Aβ1-42 and Aβ1-40, respectively, whereas monoclonal 4G8, which binds both, depleted both Aβ1-42 and Aβ1-40. The monoclonal 6E10, which selectively binds human Aβ relative to rat Aβ, depleted neither Aβ1-42 nor Aβ1-40. After immunodepletion, there was a residual signal of 16% for Aβ1-42 and 4% for Aβ1-40, averaged across depleted samples in both dose groups (Figures 7(d) and 7(e)). Thus, the residual signal appeared to be a combination of nonspecific background signal and small residual pools of ca. 15% Aβ1-42 and 7% Aβ1-40. This residual Aβ1-42 may represent either a slow turnover pool of Aβ1-42 or a source of Aβ1-42 production that is not readily inhibited by γ-secretase-targeted compounds.

To evaluate the pharmacokinetic to pharmacodynamic (PK/PD) relationship for BMS-869780 in more detail, time courses of Aβ lowering and plasma BMS-869780 concentration were carried out in mice and rats. The PK and PK/PD were then modeled sequentially using 1-compartment PK and indirect response PK/PD models, respectively. Triple transgenic mice [63] were dosed orally at 30 mg/kg or 100 mg/kg, and brain and plasma were taken from groups of animals after 3, 5, 8, 16, and 24 hours. Rats were dosed orally at 10 mg/kg, and brain and plasma were taken at the same time points as for mice. Plasma BMS-869780 showed increasing concentration until 4–8 hours then decreased (Figure 8(a)). Brain Aβ1-42 in the mouse, and both Aβ1-42 and Aβ1-40 in the rat, decreased until 8–16 hours relative to vehicle-treated groups (Figures 8(b)–8(d)). The *in vivo* plasma IC$_{50}$ values for brain Aβ1-42 were 1.9 μM and 4.0 μM for rat and mouse, respectively. After taking account of the protein bound fractions (99.5% and 99.6% in rat and mouse, resp.), these are within 2-fold factors of the *in vitro* IC$_{50}$ values of 5.1 nM and 22 nM for wild type and presenilin-1 M146V alleles, respectively (Table 1). Estimates of the PK and PD parameters are summarized in Table 2. Using the PK
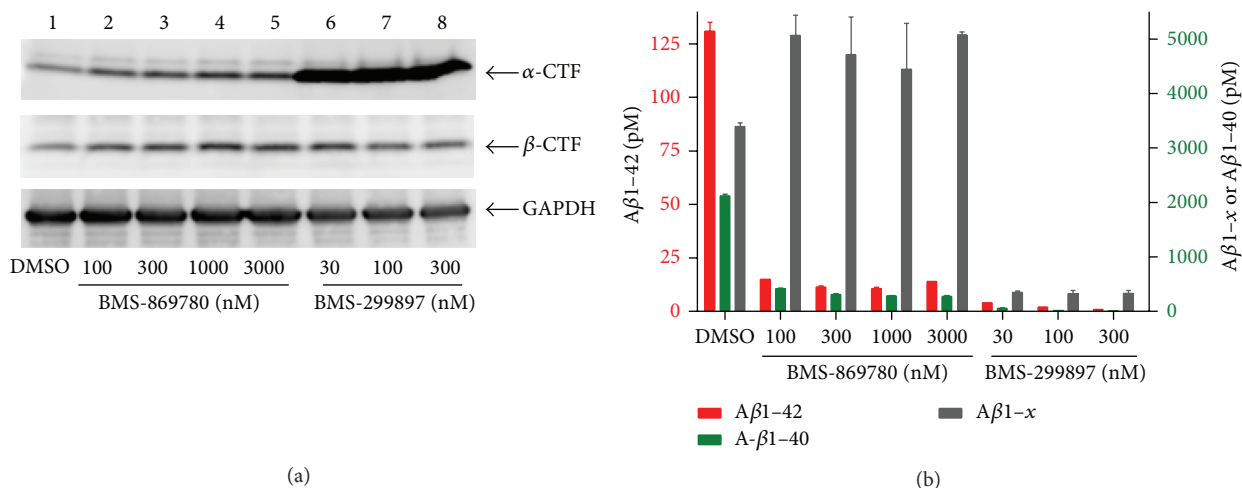
(a)

(b)

FIGURE 4: BMS-869780 had minimal effect on APP-CTF accumulation *in vitro*. H4-APPsw cell cultures were treated overnight with the indicated concentrations of BMS-869780, BMS-299897 or vehicle (0.1% DMSO). (a) Cells were harvested and analyzed by western blotting for APP-CTFα, APP-CTFβ, and GAPDH. Lane 1; culture treated with vehicle 0.1% DMSO. Lanes 2–5; cultures treated with BMS-869780 at 100 nM, 300 nM, 1000 nM, or 3000 nM, respectively. Lanes 6–8; cultures treated with BMS-299897 at 30 nM, 100 nM, or 300 nM, respectively. (b) Levels of Aβ1-42 (red; left Y-axis), Aβ1-40 (green; right Y-axis), and Aβ1-x (grey; right Y-axis) were quantified.

and PK/PD models for the rat data, steady-state assuming linear PK was predicted to occur after three daily doses, and a 3 mg/kg oral dose of BMS-869780 was predicted to yield AUC$^{24\,h}$ = 18.6 μM·h with corresponding Aβ1-42 ABEC$^{0-24\,h}$ = 26.9% at steady state. Observed and predicted values of dose, AUC, and ABEC in rat and mouse are summarized in Table 3.

3.6. Pharmacokinetics and Human Dose Prediction. To make a prediction of human PK for BMS-869780, the PK profiles for solution IV and nanoparticle suspension PO dosing of BMS-869780 were determined in rat, dog, and cynomolgus monkey (Figure 9; Table 4). Plasma exposure was readily detectable for 24 hours after dosing, and the average bioavailability of the nanoparticle suspension for the three species was 28%. Allometric scaling of the observed animal PK parameters was used to predict human PK parameters (Table 4) [70, 71]. From the predicted human PK, in combination with the PK/PD parameters from rat, a 10 mg/kg once daily dose (700 mg total) was predicted to achieve a steady-state AUC = 17.8 μM·h, C_{max} = 1.27 μM, and corresponding brain Aβ1-42 ABEC = 25% (Table 3).

3.7. Off-Targets and Safety. BMS-869780 was evaluated in a range of *in vitro* off-target activity assays. In one of these assays, pregnane-X-receptor transactivation (PXR-TA), BMS-869780 exhibited robust activity. In further experiments, BMS-869780 was shown to increase CYP3A4 mRNA expression in primary human hepatocytes. In both the PXR-TA and the primary human hepatocytes, transcription was activated at concentrations of 0.3 μM and above (Figure 10(a)), suggesting potential activation of CYP3A4 metabolism and risk for drug-drug interactions in human at the exposures predicted to lower Aβ1-42.

As a preliminary evaluation of safety *in vivo*, male and female rats were given 10, 30, and 100 mg/kg BMS-869780 orally once daily for 4 days. Endpoints included brain Aβ1-42, as described above (Figures 7(d) and 7(e)), plasma PK on day 1 and day 3 (Table 4), and histopathology for duodenum, liver, and kidney. There was no loss of exposure between day 1 and day 3, consistent with a lack of autoinduction via PXR and/or lack of BMS-869780 metabolism by CYP3A in the rat. Duodenum and kidney histology were unchanged at all dose levels. However, liver exhibited macro- and microvesicular vacuolar degeneration consistent with a fatty acid change, likely lipidosis, at all doses (Figures 10(b) and 10(c)). In the 10 mg/kg dose groups, the lowest mean AUC = 17.5 μM·h, and C_{max} = 1.9 μM, were commensurate with the target exposures determined for Aβ1-42 lowering (see Table 3). In contrast, even at the highest dose of 100 mg/kg, where exposures in excess of 200 μM·h were achieved, there was no Notch-related effect on differentiation in the duodenum.

4. Discussion

The discovery and evaluation of BMS-869780 started with a high-throughput screen of the BMS compound inventory to identify selective inhibitors of Aβ1-42 in cell cultures and ended with predictions for human dose and exposure margins for off-target activity and safety. BMS-869780 is a GSM that decreased production of the longer peptides, Aβ1-40 and Aβ1-42, and increased production of the shorter peptides, Aβ1-37 and Aβ1-38. BMS-869780 did not significantly inhibit overall levels of Aβ production, APP-CTF processing, or Notch processing.

4.1. Potency and Mechanism of BMS-869780. BMS-869780 exhibited high potency (IC$_{50}$ = 5.6 nM) for Aβ1-42 lowering in cell cultures, greater or equal in potency to the most potent
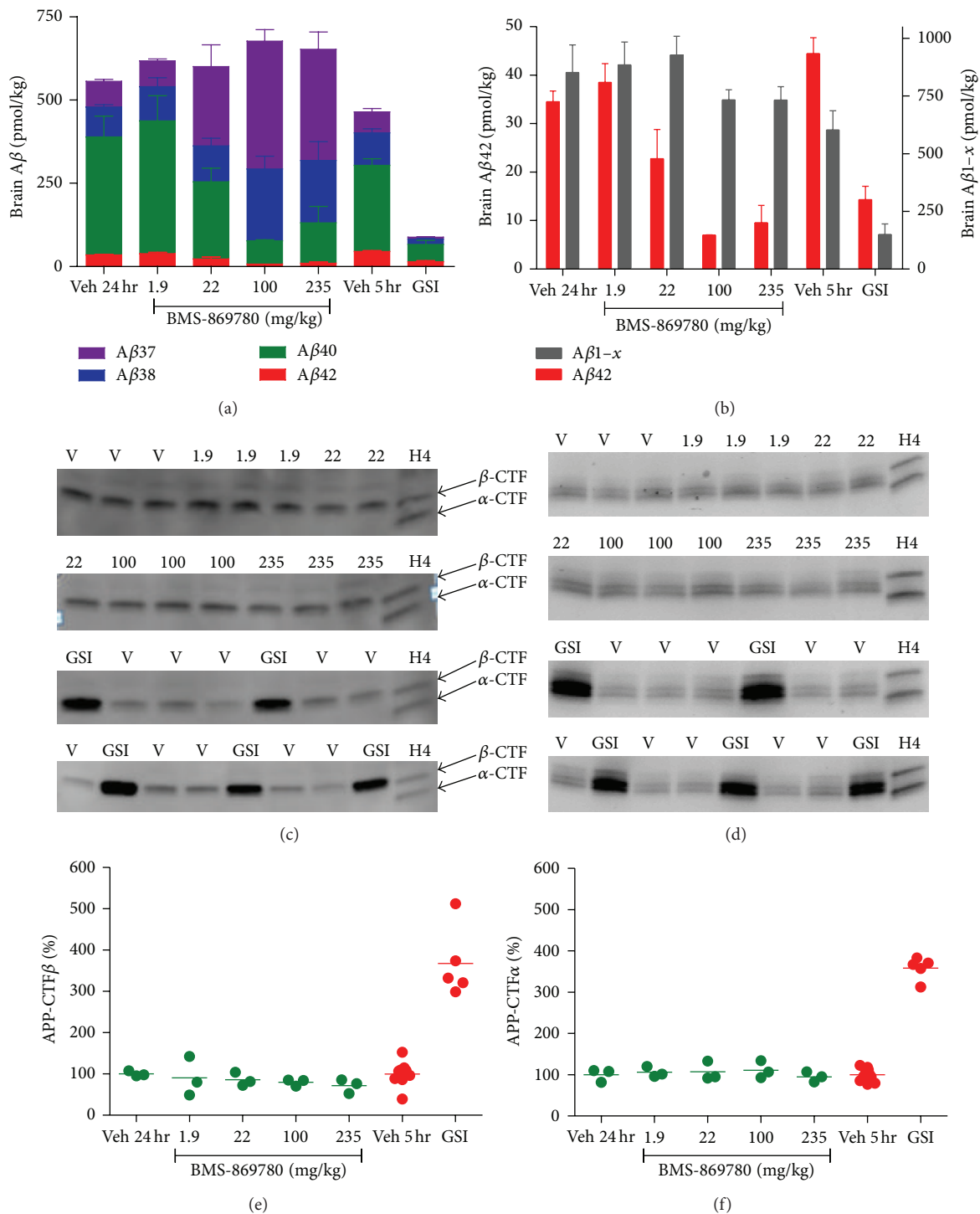
(a)

(b)

(c)

(d)

(e)

(f)

FIGURE 5: BMS-869780 modulated $A\beta$ but did not cause accumulation of βCTF or αCTF in rat brain. Rats were given oral doses of BMS-869780, and levels of brain $A\beta$, βCTF, and αCTF were determined 24 hours later. For comparison, BMS-698861 was dosed in a separate experiment and samples were taken 5 hours later. (a) Brain levels of $A\beta$1-42 (red), $A\beta$1-40 (green), $A\beta$1-38 (blue), and $A\beta$1-37 (purple) are shown as bars stacked upon one another. The total height of each bar therefore represents the sum of the four peptides. (b) $A\beta$1-42 (red—left Y axis) and $A\beta$1-x (grey—right Y axis). The same results for $A\beta$1-42 are plotted in both (a) and (b). (c) Rat brain βCTF was detected by western blotting of immunoprecipitates from samples of the same rat brains used for $A\beta$ determinations. V, vehicle groups; results from rats dosed with 1.9, 22, 100, and 235 mg/kg of BMS-869780 and 10 mg/kg BMS-698861 (GSI) are indicated. (d) Western blots of immunoprecipitated αCTF from the same rat brain samples. (e) and (f) quantification of western blots shown in (c) and (d), respectively, expressed relative to percent of average level of CTF in vehicle-treated rats. Actual doses of BMS-869780 were determined by analysis of concentrations in left-over dosing solutions.
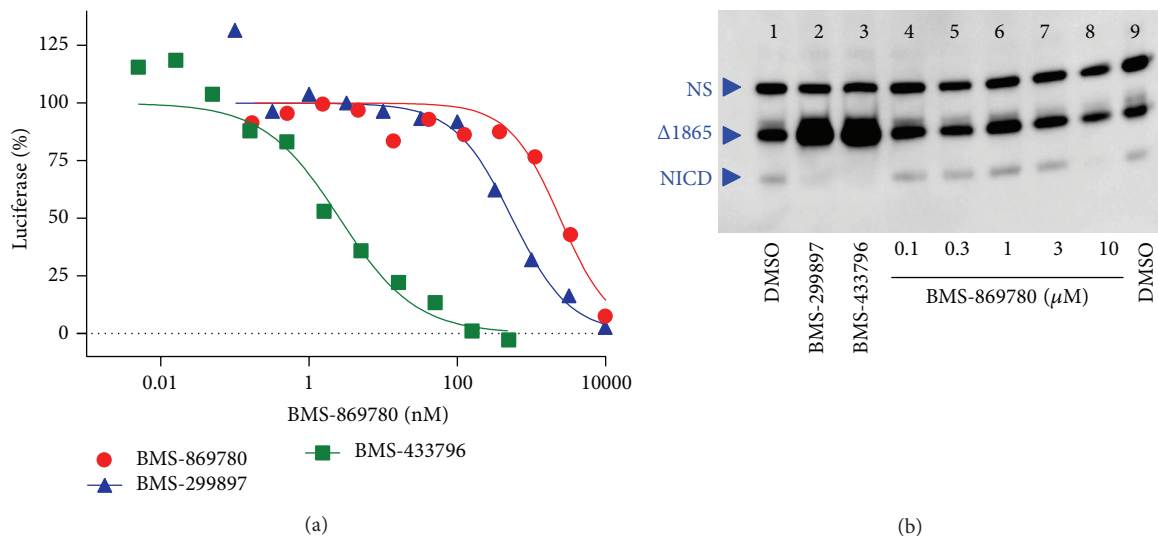
FIGURE 6: BMS-869780 did not inhibit Notch cleavage *in vitro*. (a) HeLa cell cultures were transfected with mNotchΔE and CBF1-luciferase reporter constructs, treated overnight with BMS-869780 (●), BMS-299897 (▲), or BMS-433796 (■), and luciferase assays were carried out. (b) HeLa cell cultures were transfected with mNotchΔ1865, treated with compounds overnight, and cell extracts were evaluated by western blot using anti-c-myc-HRP conjugate. Lanes 1 and 9: DMSO (0.1%) vehicle. Lane 2: BMS-299897 at 1 μM. Lane 3: BMS-433796 at 0.3 μM. Lanes 4–8: BMS-869780 at 0.1, 0.3, 1, 3, and 10 μM, respectively.

TABLE 2: PK/PD model values from mouse and rat studies.

Parameter	Units	Mouse	CV (%)	Rat	CV (%)
		PK parameters			
Kel	h^{-1}	0.28	44.1	0.10	48.4
V/F	L/kg	1.94	48.3	1.94	43.8
Ka1 (10 mg/kg)	h^{-1}			0.19	56.0
Ka1 (30 mg/kg)	h^{-1}	0.11	29.8		
Ka2 (100 mg/kg)	h^{-1}	0.046	30.0		
		PD parameters			
K_{OUT}	h^{-1}	0.72	24.9	0.48	51.4
IC$_{50}$	nM	3979	9.16	1892	26.4
$R0$	%	100	Fixed	100	Fixed
I_{max}		1	Fixed	1	Fixed
K_{in}	%/h	72	Calculated	48	Calculated

Kel-first order rate constant for drug elimination; V-volume of distribution; Ka rate constant for drug absorption; K_{OUT}-first order rate constant for degradation of Aβ1-42 or Aβ1-40; IC$_{50}$-plasma concentration required for 50% inhibition of Aβ1-42 or Aβ1-40 production; R is the response in Aβ1-42 or Aβ1-40 levels, assumed 100% at time zero, $R0$; I_{max}-range of the response of Aβ1-42 or Aβ1-40 levels; K_{in}-zero order constant for Aβ1-42 or Aβ1-40 production.

TABLE 3: Relationship between dose, plasma AUC, and Aβ ABEC.

Dose	Plasma AUC$^{0-24\,hr}$	Brain Aβ ABEC$^{24\,hr}$	
	(μM·h)	Aβ1-42 (%)	Aβ1-40 (%)
Mouse 30 mg/kg PO solution (observed 0–24 hours)	45.9	30.9	n.d.
Mouse 100 mg/kg PO solution (observed 0–24 hours)	102	55.1	n.d.
Rat 10 mg/kg PO solution (observed 0–24 hours)	46.3	47.0	46.1
Rat 3 mg/kg PO solution (predicted steady state after 3 daily doses)*	18.6	26.9	
Human 700 mg PO suspension (predicted steady state)*	17.8	25	

*Dose predicted to achieve Aβ42 ABEC of ca. 25%.
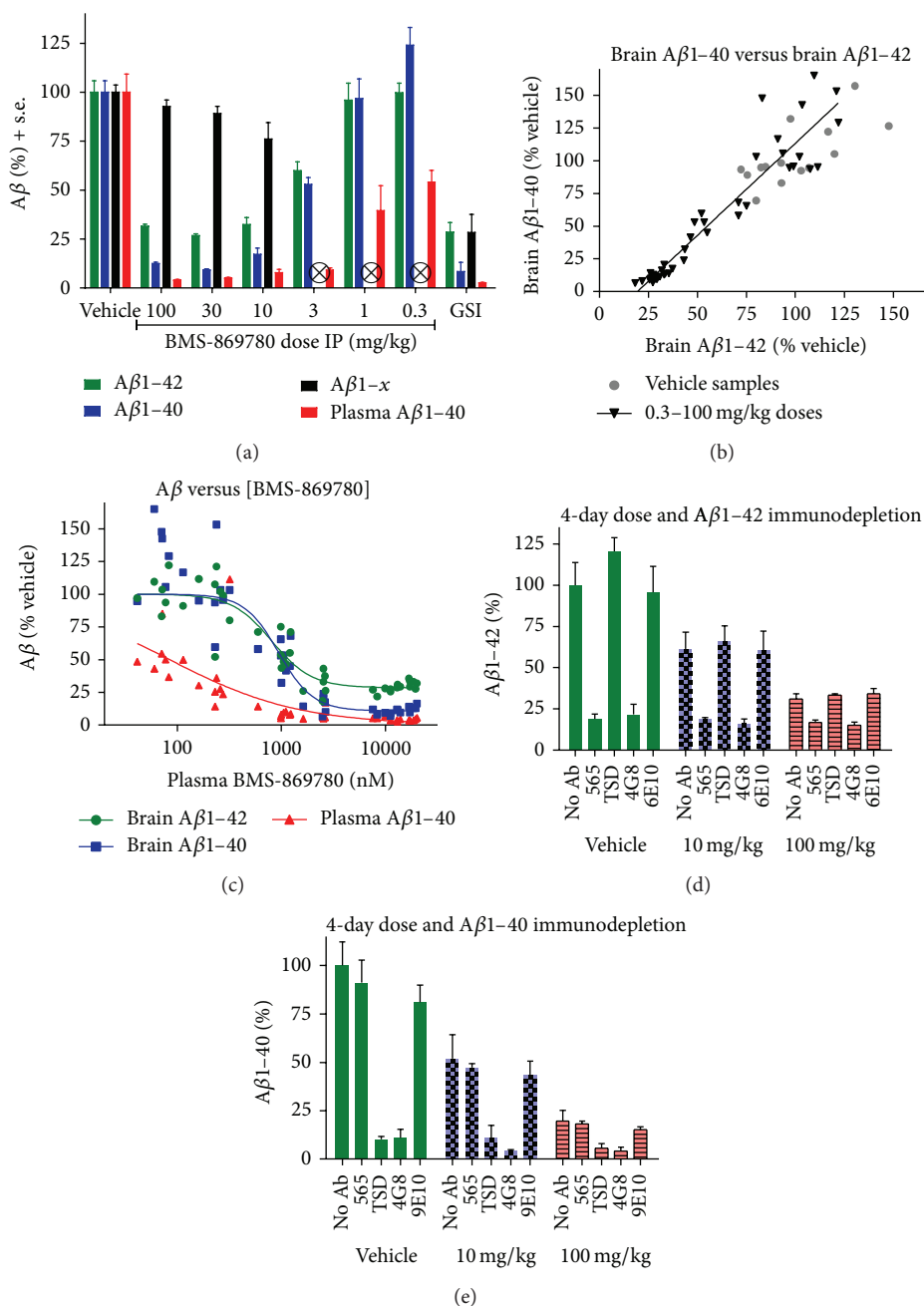
(a)

(b)

(c)

(d)

(e)

FIGURE 7: BMS-869780 dose response and evaluation of residual Aβ levels in rat brain. (a) Groups of rats received intraperitoneal (IP) injections of vehicle or BMS-869780 at doses of 100, 30, 10, 3, 1, and 0.3 mg/kg. Additional rats were dosed with GSI BMS-698861 at 30 mg/kg as a positive control for Aβ-lowering. Group sizes were seven rats for each dose of BMS-869780 and 14 rats for vehicle and GSI dose groups. Brain and plasma were harvested 5 hours after dosing. Brain Aβ1-42 (green), brain Aβ1-40 (blue), brain Aβ1-x (black), and plasma Aβ1-40 (red) were determined. Values are expressed as % relative to vehicle group mean. Whiskers represent standard error. ⊗Aβ1-x was not determined in the groups dosed at 3, 1, and 0.3 mg/kg. (b) Brain Aβ1-40 was plotted against brain Aβ1-42 for each rat dosed with BMS-869780 (black ▼) and for each rat dosed with vehicle (grey ●). Values are expressed as % relative to vehicle group mean. Whiskers represent standard error. (c) Brain Aβ1-42 (●), brain Aβ1-40 (■), and plasma Aβ1-40 (▲) were plotted against plasma concentration of BMS-869780 and the data were evaluated by fit to a four-parameter dose response curve. The top of the dose response curve was defined by vehicle group mean (100%), and the apparent IC_{50} values in terms of the plasma BMS-869780 concentration obtained for brain Aβ1-42, brain Aβ1-40, and plasma Aβ1-40 were 807 nM, 943 nM, and 84 nM, respectively. The respective 95% confidence intervals were 618–1053 nM, 704–1264 nM, and 44–158 nM. (d) Rats were dosed once daily with BMS-869780 for 4 days at 10 and 100 mg/kg or vehicle, plasma, and brain samples were taken 5 hours after the last dose, and immunodepletion of brain extracts was carried out prior to Aβ1-42 ELISA assays. Specific monoclonals used were 565 (Aβ1-42 selective), TSD (Aβ1-40 selective), 4G8 (binds both Aβ1-42 and Aβ1-40), and 6E10 (does not bind rat Aβ). After immunodepletion, Aβ1-42 was assayed by ELISA. (e) Same as described in (d), except that Aβ1-40 ELISA was carried out following the immunodepletion.

TABLE 4: Summary pharmacokinetics observed in three species and predicted in human.

		Rat	Dog	Monkey	Human predicted
IV 1 mg/kg	Clearance (mL/min/kg)	24.3 ± 1.7	5.7 ± 1.7	15.2 ± 5.9	5.6
	AUClast (nM·h)	1484 ± 121	6640 ± 2257	2632 ± 926	
	Half-life (hour)	2.0 ± 0.3	5.2 ± 1.4	4.0 ± 0.5	13
	MRT (hour)	1 ± 0.2	6.6 ± 2.0	3.8 ± 0.7	
	Vss (L/kg)	1.8 ± 0.5	2.2 ± 0.8	3.7 ± 1.3	5.2
PO suspension 5 mg/kg	AUClast (nM·h)	3995 ± 964	4546 ± 2157	2031 ± 1038	
	C_{max} (nM)	674 ± 227	487 ± 155	219 ± 94	
	T_{max} (hour)	3.3 ± 1.2	1.7 ± 0.6	2.0 ± 0	
	F (%)	54%	13%	16%	28%

MRT-mean residence time; AUClast-area under the plasma concentration-time curve from zero time until the last quantifiable concentration.

GSMs reported [39, 43, 75, 76], and was robustly active *in vivo*, capable of lowering brain Aβ1-42 and Aβ1-40 in mice and rats by 75% or more. At the same time, levels of Aβ1-37 and Aβ1-38 were increased by BMS-869780, such that overall levels of Aβ remained essentially unchanged. The effect of BMS-869780 on γ-secretase therefore does not appear to involve inhibition. To evaluate the mechanism of BMS-869780 further, APP processing intermediates were evaluated both in H4-APPsw cell cultures and in rat brain. Levels of APP-CTFβ and APP-CTFα were not affected by BMS-869780, in contrast to the GSIs BMS-698861 and BMS-299897, which caused robust accumulation. An unexpected observation emerged in the H4-APPsw cell line when it was found that GSI treatment, while causing robust APP-CTFα accumulation, did not result in APP-CTFβ accumulation. This appears to be a quirk of the H4-APPsw cell line, possibly resulting from APP-CTFβ degradation taking place predominantly through the proteasomal and lysosomal pathways, as recently reported [74]. In rat brain, γ-secretase inhibition caused robust increases in both APP-CTFα and APP-CTFβ. In contrast, while BMS-869780 caused robust decreases in Aβ1-42 and Aβ1-40, there was no effect on APP-CTFα and APP-CTFβ levels in rat brain. Thus, in the target organ, brain, BMS-869780 was demonstrated to act solely as a GSM, without inhibitory effects on γ-secretase.

The *in vivo* potency of BMS-869780 for brain Aβ1-42 lowering in rat and 3xTg mouse was evaluated in single dose time course experiments using a PK/PD indirect response model. This yielded *in vivo* IC_{50} values that were within a factor of 2-fold of the IC_{50} values for Aβ1-42 determined *in vitro*, when plasma protein binding was taken into account. In the 3xTg mouse, the *in vivo* and *in vitro* IC_{50} values were also within a factor of 2-fold when the effect of the presenilin-1 M146V allele on potency was additionally taken into account. The potency of BMS-869780 for Aβ1-42 lowering was ca. 3-fold less in cell cultures expressing the presenilin-1 M146V allele, consistent with previous reports that presenilin FAD mutants can affect the potency of GSMs [77, 78]. Thus, the *in vivo* activity of BMS-869780 in rodents corresponded well with its potency determined *in vitro*, suggesting that rodents would be predictive of activity in human.

4.2. Lack of Notch Inhibition by BMS-869780.
The lack of effect of BMS-869780 on Notch processing was demonstrated using three approaches. First, a luciferase transcriptional reporter assay for Notch1 signaling was tested in cell cultures. For BMS-869780, the ratio of Notch to Aβ1-42 IC_{50}s could not be precisely determined because of its weak activity in the Notch assays but was >1785-fold, based on an IC_{50} value >10 μM for Notch. In the same assays, GSIs exhibited a wide range of Notch/Aβ1-42 IC_{50} ratios, with values of 13 and 723 for BMS-433796 and BMS-299897, respectively (Table 1). For GSIs, it has been shown that the absolute values of Notch/Aβ1-42 IC_{50} ratios for GSIs are strongly affected by APP substrate expression levels [61], and therefore cell culture data do not translate directly to Notch/Aβ1-42 margins *in vivo*. For example, the relatively Notch-selective GSI avagacestat exhibited a Notch/Aβ1-40 IC_{50} ratio of 193 [59], but the doses that achieved Aβ lowering without Notch-related side effects were more limited *in vivo* [19]. For BMS-869780, the lack of Notch-related side effects is expected based not only on the large *in vitro* Notch/Aβ1-42 IC_{50} ratio, but also on its noninhibitory mechanism of γ-secretase modulation. In rats, BMS-869780 did not cause any histological change in duodenum, specifically a lack of goblet cell metaplasia, even after four days of dosing at high exposures. The plasma exposure of BMS-869780 achieved in this experiment was more than 12-fold above the exposure required for lowering Aβ1-42 by 25% (Aβ1-42 ABEC = 25%). A wide variety of evidence from human genetics and transgenic APP mouse models suggests lowering of Aβ1-42 by 25% would be beneficial in AD [7]. Taken together, these data support the idea that GSMs such as BMS-869780 do not cause Notch-related side effects at doses predicted to cause sufficient Aβ1-42 lowering.

4.3. Human Predictions for BMS-869780.
To predict human dose, off-target, and safety margins, the PK/PD relationship determined in rodents was used as a guide, and a target Aβ1-42 ABEC = 25% was chosen, based on evidence from rodent models that 25% might ultimately translate to a significant effect in AD [7]. The assumption that human
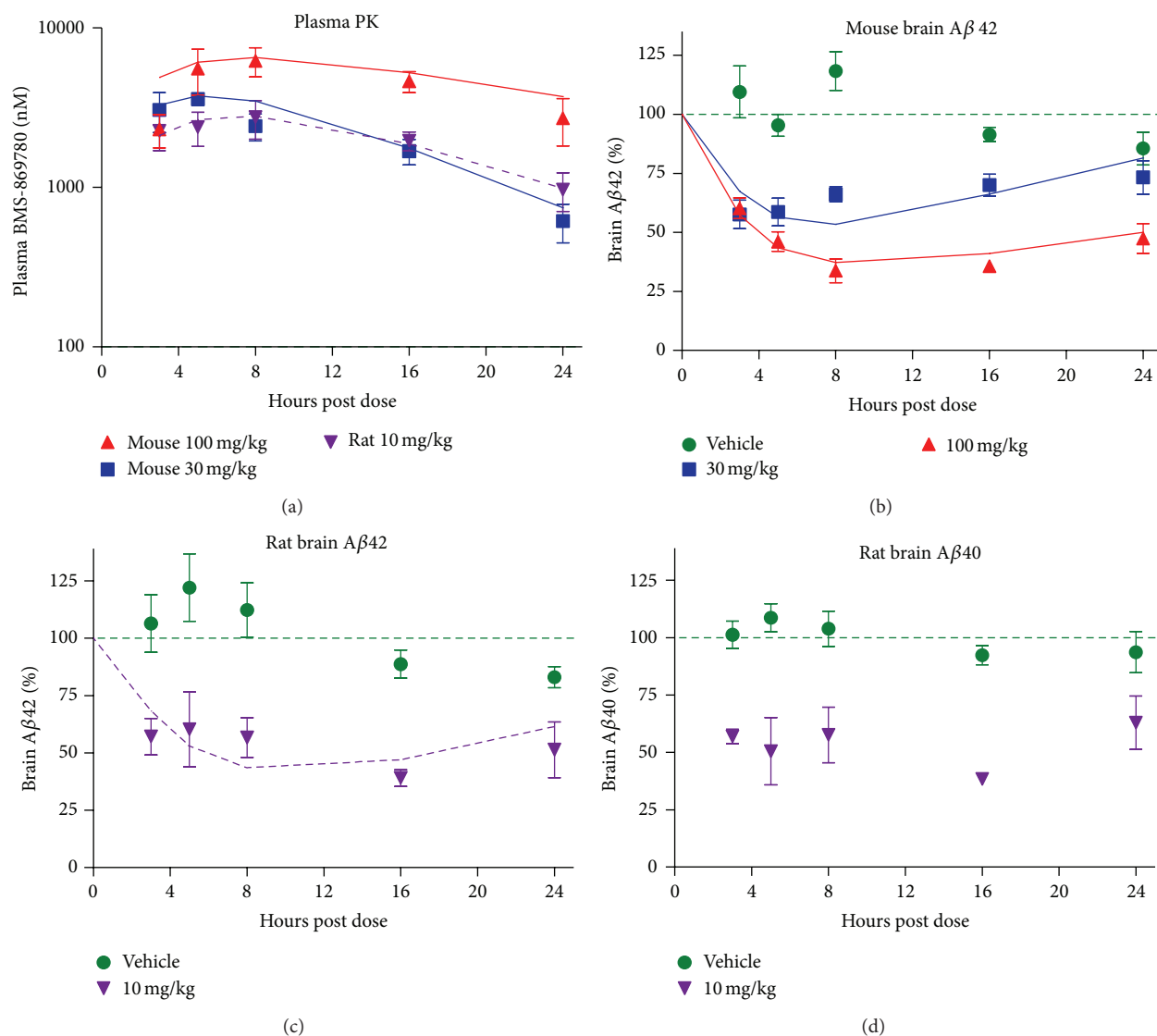
FIGURE 8: Analysis of the PK/PD relationship for BMS-869780 in rats and mice. Rats were dosed orally with BMS-869780 at 10 mg/kg, and triple transgenic mice were orally dosed at 30 mg/kg and 100 mg/kg. Additional groups of rats and mice were dosed with vehicle alone. Brain and plasma were harvested at 3, 5, 8, 16, and 24 hours after dosing for determination of brain Aβ1-42 and plasma BMS-869780 concentration. Group sizes were 5 rats or 4 mice. Whiskers represent standard error. (a) Plasma concentrations of BMS-869780 were determined for the mice dosed at 100 mg/kg (▲) and 30 mg/kg (■) and for the rats dosed at 10 mg/kg (▼). The data were fit to a one-compartment PK model and the predicted plasma BMS-869780 concentrations are shown for mouse (solid lines) and rat (broken line). (b) Brain Aβ1-42 levels were determined for the mice dosed with BMS-869780 at 100 mg/kg (▲), 30 mg/kg (■), or vehicle alone (●). The data were fitted using the indirect pharmacodynamic response model and predicted values are shown (solid lines). (c) Brain Aβ1-42 levels were determined for the rats dosed with BMS-869780 at 10 mg/kg (▼) or vehicle alone (●). The data were fitted using the indirect pharmacodynamic response model and predicted values are shown (dashed line). The values of the PK and PD parameters determined from these experiments are summarized in Table 2. (d) Brain Aβ1-40 levels determined in the same rats as illustrated in (c).

and rat PK/PD would be similar was supported by the concordance of the human *in vitro* IC$_{50}$ with the *in vivo* IC$_{50}$s determined in rat and mouse, as discussed above. The human PK parameters were then predicted through allometric scaling of PK in three species; rat, dog, and monkey, using the average bioavailability (F = 28%) achieved with a nanosuspension. The nanosuspension was chosen as a clinically relevant formulation with potential to enhance bioavailability. A dose of 700 mg was calculated to achieve

brain Aβ1-42 ABEC = 25%, with associated AUC = 17.6 μM·h and C_{max} = 1.27 μM. These AUC and C_{max} values were then used as benchmarks to compare the Aβ1-42 lowering activity against *in vivo* side effects and *in vitro* off-target activities. BMS-869780 did not cause duodenal neoplasia, the characteristic Notch-related side effect observed in rats given GSIs, even after four days dosing that achieved AUC = 316 μM·h and C_{max} = 15.5 μM (Table 5). This predicted a safety margin, specifically related to duodenal toxicity, including
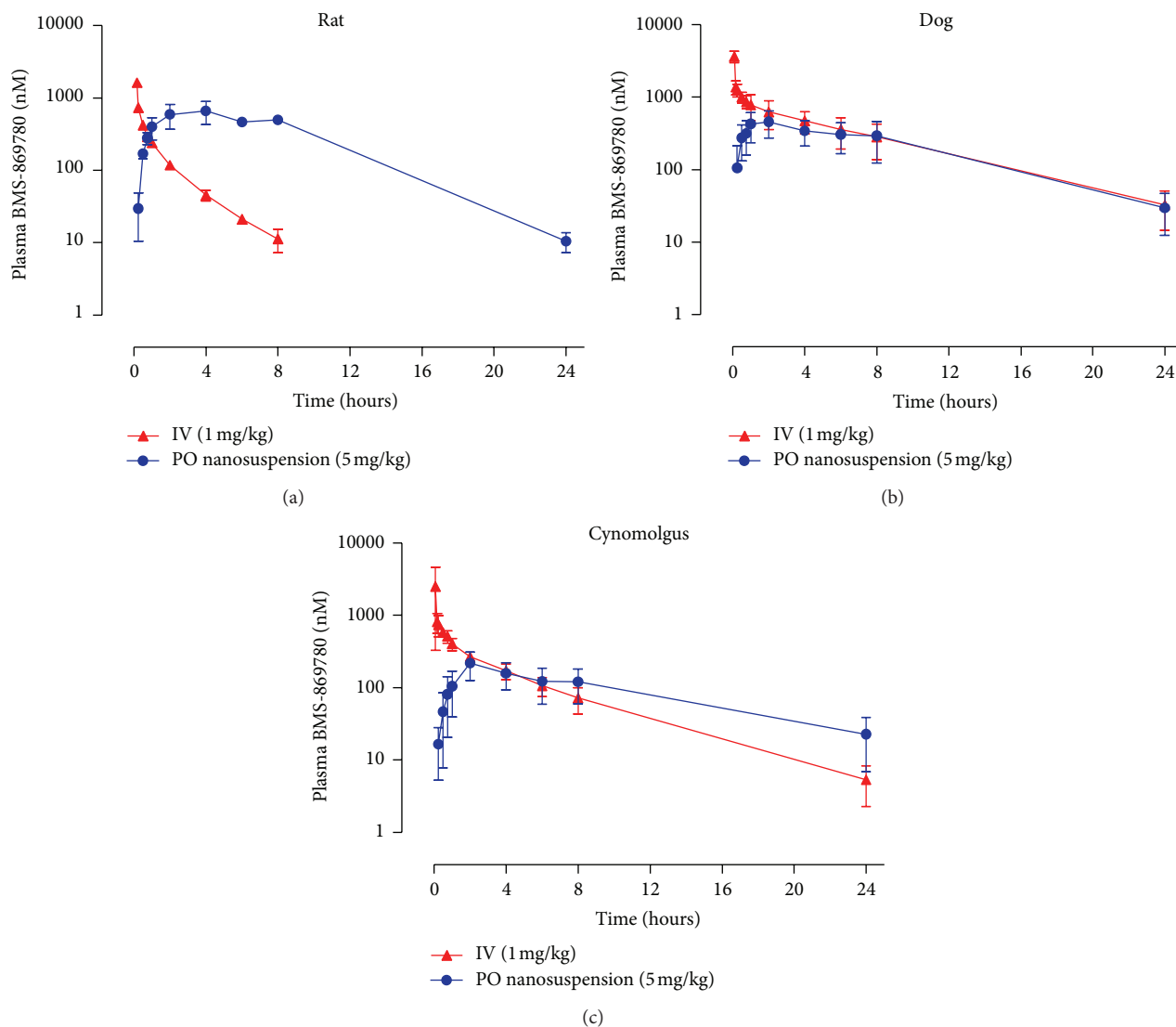
Figure 9: Pharmacokinetics (PK) of BMS-869780 across species for prediction of human PK. Rats, dogs, and cynomolgus monkeys were dosed with BMS-869780 intravenously (IV ▲) at 1 mg/kg or oral nanosuspension (PO ●) at 5 mg/kg. Plasma concentrations of BMS-869780 were determined for up to 24 hours after the dose. (a) Rat. (b) Dog. (c) Cynomolgus monkey. The derived PK parameters are summarized in Table 4.

Notch-related side effects in rat, of at least 12-fold above the Aβ1-42 lowering exposure benchmarks. On the other hand, lipidosis in the liver was observed after four daily doses of 10 mg/kg with mean C_{max} = 1.9 μM and AUC = 17.5 μM (Table 5), indicating no separation of hepatotoxicity from the Aβ1-42 lowering exposure benchmarks. Subsequent studies with other potent GSMs (not shown) did not exhibit hepatotoxicity under these conditions, suggesting an off-target mechanism of hepatotoxicity. BMS-869780 was evaluated in a wide range of *in vitro* off-target activity assays. In the case of the human PXR transcriptional reporter assay, BMS-869780 was found to be active at concentrations of 0.3 μM and above. Further experiments confirmed the activation of CYP3A4 transcription in primary human hepatocyte cultures at similar concentrations, raising the possibility of

metabolic induction and risk of drug-drug interactions at exposures required for Aβ1-42 lowering in human [79]. An overview of how experimental data were combined to determine off-target and safety margins is shown in Figure 11. In general, many GSMs exhibit poor drug-like properties, in particular high lipophilicity resulting in high active exposures and risk of systemic toxicity. Nevertheless, approaches for further optimization have been proposed, and the potential to improve drug-like properties has been demonstrated [80]. Alternatively, identification of new structural scaffolds might eventually lead to compounds with improved properties. Whether by optimization of current leads or new scaffolds, potentially the most useful guide for future compound design would be the availability of high resolution structures for GSM binding to γ-secretase.
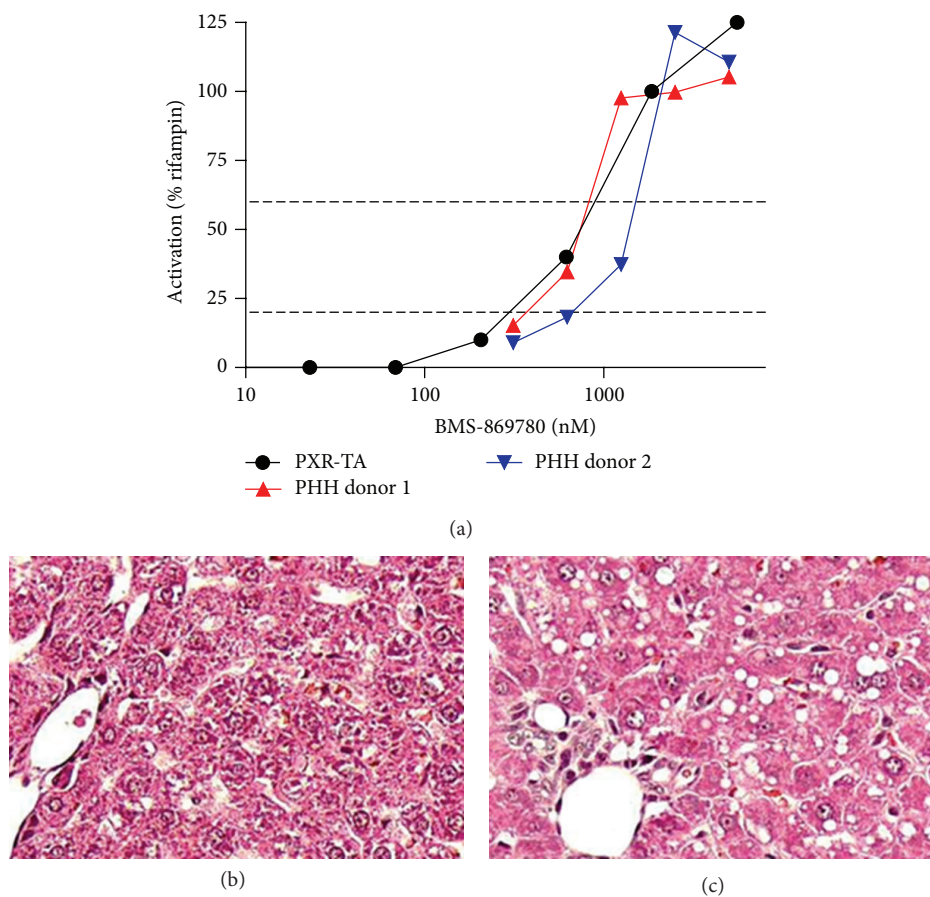
(a)

(b)

(c)

FIGURE 10: BMS-869780 caused PXR activation in vitro and lipidosis in rat liver. (a) PXR activation in the presence of BMS-869780 was evaluated in HepG2 cell cultures using a luciferase transcriptional reporter construct (●), or by assay of CYP3A4 mRNA levels in primary human hepatocyte (PHH) cultures from two individual donors (▲ and ▼). Activation in both assays is expressed as % relative to activation in the presence of rifampicin, 10 μM, in parallel cultures. (b) Liver section from vehicle-dosed rats. (c) Liver section from rats given 4 daily doses of BMS-869780 at 100 mg/kg. A summary of the plasma BMS-869780 exposures from this experiment is shown in Table 5.

TABLE 5: Summary of exposure in rat 4-day dosing experiment.

Dose (mg/kg)	Male		Female	
	Day 1	Day 3	Day 1	Day 3
		C_{max} (μM)		
10	2.0 ($\pm$0.4)	1.9 ($\pm$0.46)	2.9 ($\pm$0.4)	2.6 ($\pm$0.06)
30	6.1 ($\pm$1.8)	10.4 ($\pm$2.0)	8.2 ($\pm$1.7)	14.4 ($\pm$1.0)
100	7.7 ($\pm$0.9)	13.2 ($\pm$1.5)	10.6 ($\pm$1.0)	15.5 ($\pm$2.3)
		AUC (0–24 h) (μM·h)		
10	20.2 ($\pm$4.8)	17.5 ($\pm$5.7)	41.0 ($\pm$5.6)	25.0 ($\pm$1.5)
30	95.2 ($\pm$19.9)	128.6 ($\pm$65.0)	152.2 ($\pm$21.0)	255.1 ($\pm$28.5)
100	167.5 ($\pm$14.5)	216.9 ($\pm$80.5)	205.9 ($\pm$43.2)	316.4 ($\pm$77.0)
		T_{max} (h)		
10	5.0 ($\pm$2.0)	5.0 ($\pm$2.0)	7.0 ($\pm$2.0)	5.0 ($\pm$2.0)
30	8.0 ($\pm$0.0)	3.0 ($\pm$1.0)	5.0 ($\pm$2.0)	3.0 ($\pm$1.0)
100	19.0 ($\pm$9.0)	7.0 ($\pm$2.0)	24 ($\pm$0.0)	4.0 ($\pm$4.0)

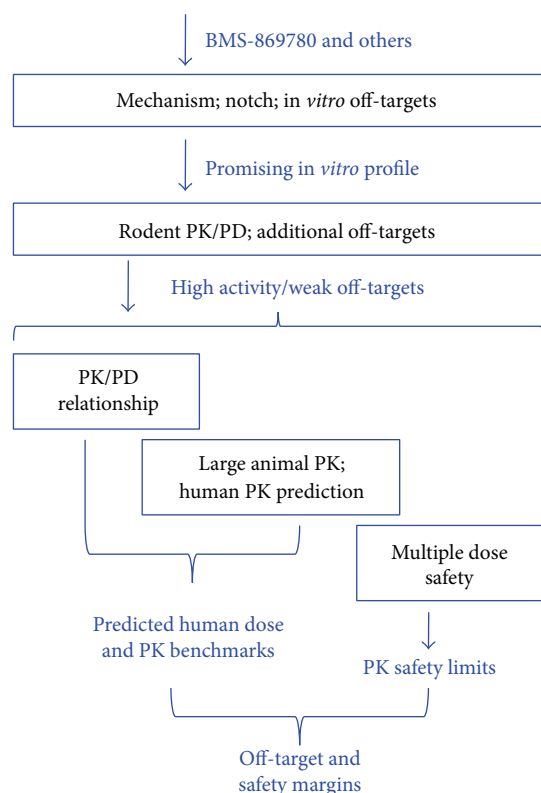| Dose (mg/kg)	Terminal concentration day 4 (μM)	
	Male	Female
10	2.4 ($\pm$0.6)	3.0 ($\pm$0.3)
30	8.9 ($\pm$1.9)	12.0 ($\pm$4.6)
100	9.2 ($\pm$3.2)	13.7 ($\pm$0.9)

FIGURE 11: An overview of the characterization of BMS-869780 illustrates only the key steps in integration of data. Additional off-target and pharmaceutics evaluations necessary for decisions on individual compounds are not represented in this diagram.

In conclusion, BMS-869780 demonstrated the potential of the GSM approach, namely, the high potency, the robust translation of activity and mechanism *in vivo*, and the absence of a Notch-related side effect after multiple days of dosing at high sustained exposures. While liver toxicity and the high predicted dose of 700 mg caused studies of BMS-869780 to be discontinued, there was no evidence to suggest that liver toxicity or PXR activation were intrinsic to the GSM mechanism. In principle, therefore, an optimal combination of sufficient potency, PK, pharmaceutical properties, and off-target profile is within reach for testing a future GSM in Alzheimer's disease.

Abbreviations

ABEC: Area between baseline and Aβ effect-time curve
AD: Alzheimer's disease
APP: β-Amyloid precursor protein
APP-CTF: β-Amyloid precursor protein C-terminal fragment
AUC: Area under the plasma concentration-time curve
CYP3A4: Cytochrome P450 3A4 isozyme
DMEM: Dulbecco's modified Eagle's medium
ELISA: Enzyme-linked immunosorbent assay
FAD: Familial Alzheimer's disease
FRET: Förster resonance energy transfer
GAPDH: Glyceraldehyde-3-phosphate dehydrogenase
GSM: γ-Secretase modulator
GSI: γ-Secretase inhibitor
HTS: High-throughput screen
KO: Knockout (gene ablation)
dKO: Double knockout (gene ablation)
MEF: Mouse embryonic fibroblast
MRT: Mean residence time
NICD: Notch intracellular domain
PD: Pharmacodynamics
PK: Pharmacokinetics
PK/PD: Pharmacokinetic/pharmacodynamic relationship
PXR-TA: Pregnane-X-receptor transactivation assay
SEAP: Secreted alkaline phosphatase.

Conflict of Interests

All the authors are employees or former employees of Bristol-Myers Squibb.

References

[1] A. Wimo and M. Prince, "The global economic impact of dementia," Alzheimer's Disease International World Alzheimer Report 2010, 2010.

[2] M. Prince, R. Bryce, and C. Ferri, "The benefits of early diagnosis and intervention," Alzheimer's Disease International World Alzheimer Report 2011, 2011.

[3] M. A. Findeis, "The role of amyloid β peptide 42 in Alzheimer's disease," *Pharmacology & Therapeutics*, vol. 116, no. 2, pp. 266–286, 2007.

[4] J. Hardy and D. J. Selkoe, "The amyloid hypothesis of Alzheimer's disease: progress and problems on the road to therapeutics," *Science*, vol. 297, no. 5580, pp. 353–356, 2002.

[5] E. Karran, M. Mercken, and B. de Strooper, "The amyloid cascade hypothesis for Alzheimer's disease: an appraisal for the development of therapeutics," *Nature Reviews Drug Discovery*, vol. 10, no. 9, pp. 698–712, 2011.

[6] C. Haass, "Take five—BACE and the γ-secretase quartet conduct Alzheimer's amyloid β-peptide generation," *The EMBO Journal*, vol. 23, no. 3, pp. 483–488, 2004.

[7] J. H. Toyn and M. K. Ahlijanian, "Interpreting Alzheimer's disease clinical trials in light of the effects on amyloid-β," *Alzheimer's Research & Therapy*, vol. 6, article 14, 2014.

[8] M. S. Wolfe, W. Xia, B. L. Ostaszewski, T. S. Diehl, W. T. Kimberly, and D. J. Selkoe, "Two transmembrane aspartates in presenilin-1 required for presenilin endoproteolysis and γ-secretase activity," *Nature*, vol. 398, no. 6727, pp. 513–517, 1999.

[9] J. Lundqvist and J. Näslund, "γ-Secretase: a complex target for Alzheimer's disease," *Current Opinion in Pharmacology*, vol. 7, pp. 112–118, 2007.

[10] V. K. Lazarov, P. C. Fraering, W. Ye, M. S. Wolfe, D. J. Selkoe, and H. Li, "Electron microscopic structure of purified, active γ-secretase reveals an aqueous intramembrane chamber and two pores," *Proceedings of the National Academy of Sciences of the United States of America*, vol. 103, no. 18, pp. 6889–6894, 2006.

[11] P. Osenkowski, H. Li, W. Ye et al., "Cryoelectron microscopy structure of purified γ-secretase at 12 Å resolution," *Journal of Molecular Biology*, vol. 385, no. 2, pp. 642–652, 2009.

[12] F. Renzi, X. Zhang, W. J. Rice et al., "Structure of γ-secretase and its trimeric pre-activation intermediate by single-particle electron microscopy," *The Journal of Biological Chemistry*, vol. 286, no. 24, pp. 21440–21449, 2011.

[13] C. Sato, Y. Morohashi, T. Tomita, and T. Iwatsubo, "Structure of the catalytic pore of γ-secretase probed by the accessibility of substituted cysteines," *The Journal of Neuroscience*, vol. 26, no. 46, pp. 12081–12088, 2006.

[14] T. Sato, T. S. Diehl, S. Narayanan et al., "Active γ-secretase complexes contain only one of each component," *The Journal of Biological Chemistry*, vol. 282, no. 47, pp. 33985–33993, 2007.

[15] X. Li, S. Dang, C. Yan, X. Gong, J. Wang, and Y. Shi, "Structure of a presenilin family intramembrane aspartate protease," *Nature*, vol. 493, no. 7430, pp. 56–61, 2013.

[16] A. Haapasalo and D. M. Kovacs, "The many substrates of presenilin/γ-secretase," *Journal of Alzheimer's Disease*, vol. 25, no. 1, pp. 3–28, 2011.

[17] J. Milano, J. McKay, C. Dagenais et al., "Modulation of Notch processing by γ-secretase inhibitors causes intestinal goblet cell metaplasia and induction of genes known to specify gut secretory lineage differentiation," *Toxicological Sciences*, vol. 82, no. 1, pp. 341–358, 2004.

[18] G. T. Wong, D. Manfra, F. M. Poulet et al., "Chronic treatment with the γ-secretase inhibitor LY-411,575 inhibits γ-amyloid peptide production and alters lymphopoiesis and intestinal cell differentiation," *The Journal of Biological Chemistry*, vol. 279, no. 13, pp. 12876–12882, 2004.

[19] C. F. Albright, R. Dockens, J. E. Meredith Jr. et al., "Pharmacodynamics of selective inhibition of γ-secretase by avagacestat," *Journal of Pharmacology and Experimental Therapeutics*, vol. 344, no. 3, pp. 686–695, 2013.

[20] C. J. Crump, B. A. Fish, S. V. Castro et al., "Piperidine acetic acid based γ-secretase modulators directly bind to presenilin-1," *ACS Chemical Neuroscience*, vol. 2, no. 12, pp. 705–710, 2011.

[21] A. Ebke, T. Luebbers, A. Fukumori et al., "Novel γ-secretase enzyme modulators directly target presenilin protein," *The Journal of Biological Chemistry*, vol. 286, no. 43, pp. 37181–37186, 2011.

[22] Y. Ohki, T. Higo, K. Uemura et al., "Phenylpiperidine-type γ-secretase modulators target the transmembrane domain 1 of presenilin 1," *The EMBO Journal*, vol. 30, no. 23, pp. 4815–4824, 2011.

[23] T. Jumpertz, A. Rennhack, J. Ness et al., "Presenilin is the molecular target of acidic γ-secretase modulators in living cells," *PLoS ONE*, vol. 7, no. 1, article e30484, 2012.

[24] N. Pozdnyakov, H. E. Murrey, C. J. Crump et al., "γ-Secretase modulator (GSM) photoaffinity probes reveal distinct allosteric binding sites on presenilin," *The Journal of Biological Chemistry*, vol. 288, no. 14, pp. 9710–9720, 2013.

[25] B. Tate, T. D. McKee, R. M. B. Loureiro et al., "Modulation of gamma-secretase for the treatment of Alzheimer's disease," *International Journal of Alzheimer's Disease*, vol. 2012, Article ID 210756, 10 pages, 2012.

[26] M. Okochi, A. Fukumori, J. Jiang et al., "Secretion of the Notch-1 Aβ-like peptide during Notch signaling," *The Journal of Biological Chemistry*, vol. 281, no. 12, pp. 7890–7898, 2006.

[27] M. Okochi, H. Steiner, A. Fukumori et al., "Presenilins mediate a dual intramembranous γ-secretase cleavage of Notch-1," *The EMBO Journal*, vol. 21, no. 20, pp. 5408–5416, 2002.

[28] S. Weggen, J. L. Eriksen, P. Das et al., "A subset of NSAIDs lower amyloidogenic Aβ42 independently of cyclooxygenase activity," *Nature*, vol. 414, no. 6860, pp. 212–216, 2001.

[29] M. Takami, Y. Nagashima, Y. Sano et al., "γ-Secretase: successive tripeptide and tetrapeptide release from the transmembrane domain of β-carboxyl terminal fragment," *The Journal of Neuroscience*, vol. 29, no. 41, pp. 13042–13052, 2009.

[30] M. Takami and S. Funamoto, "γ-Secretase-dependent proteolysis of transmembrane domain of amyloid precursor protein: successive tri-and tetrapeptide release in amyloid β-protein production," *International Journal of Alzheimer's Disease*, vol. 2012, Article ID 591392, 7 pages, 2012.

[31] T. Sato, N. Dohmae, Y. Qi et al., "Potential link between amyloid β-protein 42 and C-terminal fragment γ 49-99 of β-amyloid precursor protein," *The Journal of Biological Chemistry*, vol. 278, no. 27, pp. 24294–20301, 2003.

[32] L. Chávez-Gutiérrez, L. Bammens, I. Benilova et al., "The mechanism of γ-secretase dysfunction in Alzheimer's disease," *The EMBO Journal*, vol. 31, no. 10, pp. 2261–2274, 2012.

[33] J. L. Eriksen, S. A. Sagi, T. E. Smith et al., "NSAIDs and enantiomers of flurbiprofen target γ-secretase and lower Aβ42 in vivo," *The Journal of Clinical Investigation*, vol. 112, no. 3, pp. 440–449, 2003.

[34] T. Kukar, S. Prescott, J. L. Eriksen et al., "Chronic administration of R-flurbiprofen attenuates learning impairments in transgenic amyloid precursor protein mice," *BMC Neuroscience*, vol. 8, article 54, 2007.

[35] D. R. Galasko, N. Graff-Radford, S. May et al., "Safety, tolerability, pharmacokinetics, and Aβ levels after short-term administration of R-flurbiprofen in healthy elderly individuals," *Alzheimer Disease & Associated Disorders*, vol. 21, no. 4, pp. 292–299, 2007.

[36] K. Nakano-Ito, Y. Fujikawa, T. Hihara et al., "E2012-induced cataract and its predictive biomarkers," *Toxicological Sciences*, vol. 137, no. 1, pp. 249–258, 2014.

[37] Y. Yu, V. Logovinsky, E. Schuck et al., "Safety, tolerability, pharmacokinetics, and pharmacodynamics of the novel γ-secretase modulator, E2212, in healthy human subjects," *The Journal of Clinical Pharmacology*, vol. 54, no. 5, pp. 528–536, 2014.

[38] J. P. Caldwell, C. E. Bennett, T. M. McCracken et al., "Iminoheterocycles as γ-secretase modulators," *Bioorganic & Medicinal Chemistry Letters*, vol. 20, no. 18, pp. 5380–5384, 2010.

[39] M. Z. Kounnas, A. M. Danks, S. Cheng et al., "Modulation of γ-secretase reduces β-amyloid deposition in a transgenic mouse model of Alzheimer's disease," *Neuron*, vol. 67, no. 5, pp. 769–780, 2010.

[40] M. G. Stanton, J. Hubbs, D. Sloman et al., "Fluorinated piperidine acetic acids as γ-secretase modulators," *Bioorganic & Medicinal Chemistry Letters*, vol. 20, no. 2, pp. 755–758, 2010.

[41] J. Hawkins, D. C. Harrison, S. Ahmed et al., "Dynamics of Aβ42 reduction in plasma, CSF and brain of rats treated with the γ-secretase modulator, GSM-10h," *Neurodegenerative Diseases*, vol. 8, no. 6, pp. 455–464, 2011.

[42] I. Hussain, D. C. Harrison, J. Hawkins et al., "TASTPM mice expressing amyloid precursor protein and presenilin-1 mutant transgenes are sensitive to γ-secretase modulation and amyloid-β42 lowering by GSM-10h," *Neurodegenerative Diseases*, vol. 8, no. 1-2, pp. 15–24, 2011.

[43] T. Li, Y. Huang, S. Jin et al., "γ-Secretase modulators do not induce Aβ-rebound and accumulation of β-C-terminal fragment," *Journal of Neurochemistry*, vol. 121, no. 2, pp. 277–286, 2012.

[44] H. Peng, T. Talreja, Z. Xin et al., "Discovery of BIIB042, a potent, selective, and orally bioavailable γ-secretase modulator," *ACS Medicinal Chemistry Letters*, vol. 2, no. 10, pp. 786–791, 2011.

[45] B. van Broeck, J.-M. Chen, G. Tréton et al., "Chronic treatment with a novel γ-secretase modulator, JNJ-40418677, inhibits amyloid plaque formation in a mouse model of Alzheimer's disease," *British Journal of Pharmacology*, vol. 163, no. 2, pp. 375–389, 2011.

[46] Z. Wan, A. Hall, Y. Sang et al., "Pyridine-derived γ-secretase modulators," *Bioorganic & Medicinal Chemistry Letters*, vol. 21, no. 16, pp. 4832–4835, 2011.

[47] T. Borgegard, A. Juréus, F. Olsson et al., "First and second generation γ-secretase modulators (GSMs) modulate amyloid-β (Aβ) peptide production through different mechanisms," *The Journal of Biological Chemistry*, vol. 287, no. 15, pp. 11810–11819, 2012.

[48] Y. Mitani, J. Yarimizu, K. Saita et al., "Differential effects between γ-secretase inhibitors and modulators on cognitive function in amyloid precursor protein-transgenic and non-transgenic mice," *The Journal of Neuroscience*, vol. 32, no. 6, pp. 2037–2050, 2012.

[49] Z.-Y. Sun, T. Asberom, T. Bara et al., "Cyclic hydroxyamidines as amide isosteres: discovery of oxadiazolines and oxadiazines as potent and highly efficacious γ-secretase modulators *in vivo*," *Journal of Medicinal Chemistry*, vol. 55, no. 1, pp. 489–502, 2012.

[50] Y. Huang, T. Li, A. Eatherton et al., "Orally bioavailable and brain-penetrant pyridazine and pyridine-derived γ-secretase modulators reduced amyloidogenic Aβ peptides *in vivo*," *Neuropharmacology*, vol. 70, pp. 278–286, 2013.

[51] R. M. Loureiro, J. A. Dumin, T. D. McKee et al., "Efficacy of SPI-1865, a novel gamma-secretase modulator, in multiple rodent models," *Alzheimer's Research & Therapy*, vol. 5, no. 2, article 19, 2013.

[52] K. Rogers, K. M. Felsenstein, L. Hrdlicka et al., "Modulation of γ-secretase by EVP-0015962 reduces amyloid deposition and behavioral deficits in Tg2576 mice," *Molecular Neurodegeneration*, vol. 7, no. 1, article 61, 2012.

[53] Y. Mitani, J. Yarimizu, H. Akashiba, Y. Shitaka, K. Ni, and N. Matsuoka, "Amelioration of cognitive deficits in plaque-bearing Alzheimer's disease model mice through selective reduction of nascent soluble Aβ 42 without affecting other Aβ pools," *Journal of Neurochemistry*, vol. 125, no. 3, pp. 465–472, 2013.

[54] L. R. Marcin, L. A. Thompson III, K. M. Boy et al., "Bicyclic compounds for the reduction of beta-amyloid production," Bristol-Myers Squibb US20110015175, WO2010083141, 2010.

[55] L. R. Marcin, M. A. Higgins, K. A. Lentz et al., "Bicyclic triazoles as modulators of γ-secretase for the treatment of Alzheimer's disease," in *Proceedings of the 243rd ACS National Meeting & Exposition*, San Diego, Calif, USA, March 2012.

[56] D. M. Barten, V. L. Guss, A. Corsa et al., "Dynamics of β-amyloid reductions in brain, cerebrospinal fluid, and plasma of β-amyloid precursor protein transgenic mice treated with a γ-secretase inhibitor," *Journal of Pharmacology and Experimental Therapeutics*, vol. 312, no. 2, pp. 635–643, 2005.

[57] C. V. C. Prasad, M. Zheng, S. Vig et al., "Discovery of (*S*)-2-((*S*)-2-(3,5-difluorophenyl)-2-hydroxyacetamido)-*N*-((*S*,*Z*)-3-methyl-4-oxo-4,5-dihydro-3*H*-benzo[*d*][1,2]diazepin-5-yl)propanamide (BMS-433796): A γ-secretase inhibitor with Aβ lowering activity in a transgenic mouse model of Alzheimer's disease," *Bioorganic & Medicinal Chemistry Letters*, vol. 17, no. 14, pp. 4006–4011, 2007.

[58] P. J. Gilligan, "Sulfonamide bicyclic compounds," Bristol-Myers Squibb US20067144894, WO2006034480, 2005.

[59] K. Gillman, J. E. Starrett Jr., M. F. Parker et al., "Discovery and evaluation of BMS-708163, a potent, selective and orally bioavailable γ-secretase inhibitor," *ACS Medicinal Chemistry Letters*, vol. 1, no. 3, pp. 120–124, 2010.

[60] A. Herreman, D. Hartmann, W. Annaert et al., "Presenilin 2 deficiency causes a mild pulmonary phenotype and no changes in amyloid precursor protein processing but enhances the embryonic lethal phenotype of presenilin 1 deficiency," *Proceedings of the National Academy of Sciences of the United States of America*, vol. 96, no. 21, pp. 11872–11877, 1999.

[61] C. R. Burton, J. E. Meredith, D. M. Barten et al., "The amyloid-β rise and γ-secretase inhibitor potency depend on the level of substrate expression," *The Journal of Biological Chemistry*, vol. 283, no. 34, pp. 22992–23003, 2008.

[62] S. Sankaranarayanan, E. A. Price, G. Wu et al., "*In vivo* β-secretase 1 inhibition leads to brain Aβ lowering and increased α-secretase processing of amyloid precursor protein without effect on neuregulin-1," *Journal of Pharmacology and Experimental Therapeutics*, vol. 324, no. 3, pp. 957–969, 2008.

[63] S. Oddo, A. Caccamo, J. D. Shepherd et al., "Triple-transgenic model of Alzheimer's disease with plaques and tangles: intracellular Aβ and synaptic dysfunction," *Neuron*, vol. 39, no. 3, pp. 409–421, 2003.

[64] T. A. Lanz and J. B. Schachter, "Demonstration of a common artifact in immunosorbent assays of brain extracts: development of a solid-phase extraction protocol to enable measurement of amyloid-β from wild-type rodent brain," *Journal of Neuroscience Methods*, vol. 157, no. 1, pp. 71–81, 2006.

[65] J. H. Toyn, X.-A. Lin, M. W. Thompson et al., "Viable mouse gene ablations that robustly alter brain Aβ levels are rare," *BMC Neuroscience*, vol. 11, article 143, 2010.

[66] H.-W. Klafki, J. Wiltfang, and M. Staufenbiel, "Electrophoretic separation of βA4 peptides (1–40) and (1–42)," *Analytical Biochemistry*, vol. 237, no. 1, pp. 24–29, 1996.

[67] R. Kopan, E. H. Schroeter, H. Weintraub, and J. S. Nye, "Signal transduction by activated mNotch: importance of proteolytic processing and its regulation by the extracellular domain," *Proceedings of the National Academy of Sciences of the United States of America*, vol. 93, no. 4, pp. 1683–1688, 1996.

[68] Y. Blat, J. E. Meredith, Q. Wang et al., "Mutations at the P1′ position of Notch1 decrease intracellular domain stability rather

than cleavage by γ-secretase," *Biochemical and Biophysical Research Communications*, vol. 299, no. 4, pp. 569–573, 2002.

[69] N. L. Dayneka, V. Garg, and W. J. Jusko, "Comparison of four basic models of indirect pharmacodynamic responses," *Journal of Pharmacokinetics and Biopharmaceutics*, vol. 21, no. 4, pp. 457–478, 1993.

[70] I. Mahmood, "Application of allometric principles for the prediction of pharmacokinetics in human and veterinary drug development," *Advanced Drug Delivery Reviews*, vol. 59, no. 11, pp. 1177–1192, 2007.

[71] J. Mordenti and W. Chappell, "The use of interspecies scaling in toxicokinetics," in *Toxicokinetics and Drug Development*, pp. 42–96, Pergamon Press, New York, NY, USA, 1989.

[72] B. Goodwin, E. Hodgson, and C. Liddle, "The orphan human pregnane X receptor mediates the transcriptional activation of CYP3A4 by rifampicin through a distal enhancer module," *Molecular Pharmacology*, vol. 56, no. 6, pp. 1529–1539, 1999.

[73] W. Li, "A fast clustering algorithm for analyzing highly similar compounds of very large libraries," *Journal of Chemical Information and Modeling*, vol. 46, no. 5, pp. 1919–1923, 2006.

[74] H. A. Bustamante, A. Rivera-Diccter, V. A. Cavieres et al., "Turnover of C99 is controlled by a crosstalk between ERAD and ubiquitin-independent lysosomal degredation in human neuroglioma cells," *PLoS ONE*, vol. 8, no. 12, article e83096, 2013.

[75] H. Borghys, M. Tuefferd, B. van Broeck et al., "A canine model to evaluate efficacy and safety of γ-secretase inhibitors and modulators," *Journal of Alzheimer's Disease*, vol. 28, no. 4, pp. 809–822, 2012.

[76] J. Qin, W. Zhou, X. Huang et al., "Discovery of a potent pyrazolopyridine series of γ-secretase modulators," *ACS Medicinal Chemistry Letters*, vol. 2, no. 6, pp. 471–476, 2011.

[77] R. M. Page, K. Baumann, M. Tomioka et al., "Generation of Aβ38 and Aβ42 is independently and differentially affected by familial Alzheimer disease-associated presenilin mutations and γ-secretase modulation," *The Journal of Biological Chemistry*, vol. 283, no. 2, pp. 677–683, 2008.

[78] B. Kretner, A. Fukumori, A. Gutsmiedl et al., "Attenuated Aβ42 responses to low potency γ-secretase modulators can be overcome for many pathogenic presenilin mutants by second-generation compounds," *The Journal of Biological Chemistry*, vol. 286, no. 17, pp. 15240–15251, 2011.

[79] M. W. Sinz, "Pregnane X receptor: "prediction and attenuation of human CYP3A4 enzyme induction and drug-drug interactions"," *Annual Reports in Medicinal Chemistry*, vol. 43, pp. 405–418, 2008.

[80] H. J. M. Gijsen and M. Mercken, "γ-Secretase modulators: can we combine potency with safety?" *International Journal of Alzheimer's Disease*, vol. 2012, Article ID 295207, 10 pages, 2012.